Dominant negative Ras (DN Ras) attenuates pathological ventricular remodeling in pressure overload cardiac hypertrophy

Manuel Ramos-Kuri, Kleopatra Rapti, Hind Mehel, Shihong Zhang, Perundurai S Dhandapany, Lifan Liang, Alejandro Garcia-Carranca, Regis Bobe, Rodolphe Fischmeister, Serge Adnot, et al.

Dominant negative Ras (DN Ras) attenuates pathological ventricular remodeling in pressure overload cardiac hypertrophy.

Manuel Ramos-Kuri[1,3,4,5,6], Kleopatra Rapti[1#], Hind Mehel[9#], Shihong Zhang[1], Perundurai S. Dhandapany[2], Lifan Liang[1,4], Alejandro García-Carrancá[6], Regis Bobe[8], Rodolphe Fischmeister[9], Serge Adnot[1,7], Djamel Lebeche[1,4], Roger J. Hajjar[1,4], Larissa Lipskaia[1,7*], Elie R. Chemaly[1,4*].

(1) Cardiovascular Research Center, Icahn School of Medicine at Mount Sinai, New York, NY 10029, USA. (present address for DL, LL and RJH).

(2) Center for Molecular Cardiology, Icahn School of Medicine at Mount Sinai, New York, NY 10029, USA.

(3) Centro de Investigación Social Avanzada. Querétaro. México (present address for MRK)

(4) Cardiovascular Research Center, Massachusetts General Hospital, Charlestown, MA, USA.

(5) Laboratorio de Biología Molecular, Universidad Panamericana, México.

(6) Instituto de Investigaciones Biomédicas, Universidad Nacional Autónoma de México

(7) INSERM U955 and Département de Physiologie, Hôpital Henri Mondor, AP-HP, 94010, Créteil, France; Université Paris-Est Créteil (UPEC), France

(8) INSERM U770; Université Paris Sud, Le Kremlin-Bicêtre, France

(9) UMR-S 1180 - LabEx LERMIT DHU TORINO - SFR IPSIT Faculté de Pharmacie Université Paris-Sud 5, Châtenay-Malabry, France.

# HM and KR contributed equally to this work.

*LL and ERC contributed equally to this work.

Corresponding author:

Manuel Ramos-Kuri
Centro de Investigación Social Avanzada. México
Avenida Fray Luis de Leon No. 1000
CP 76190. Querétaro, México
E-mail: manuel.ramos@cisav.org

ABSTRACT

The importance of the oncogene Ras in cardiac hypertrophy is well appreciated. The hypertrophic effects of the constitutively active mutant Ras-Val12 are revealed by clinical syndromes due to the Ras mutations and experimental studies. We examined the possible anti-hypertrophic effect of Ras inhibition *in vitro* using rat neonatal cardiomyocytes (NRCM) and *in vivo* in the setting of pressure-overload left ventricular (LV) hypertrophy (POH) in rats. Ras functions were modulated via adenovirus directed gene transfer of active mutant Ras-Val12 or dominant negative mutant N17-DN-Ras. Ras-Val12 expression *in vitro* activates NFAT resulting in pro-hypertrophic and cardio-toxic effects on NRCM beating and Z-line organization. In contrast, the N17-DN-Ras was antihypertrophic on NRCM, inhibited NFAT and exerted cardio-protective effects attested by preserved NRCM beating and Z line structureAdditional experiments demonstrated the antihypertrophic effects of siRNA-H-Ras on NRCM. In POH, both Ras mutants were associated with similar hypertrophy two weeks after simultaneous induction of POH and Ras-mutant gene transfer. However, LV diameters were higher and LV fractional shortening lower in the Ras-Val12 group compared to control and DN-Ras. Moreover, N17-DN-Ras reduced the cross-sectional area of cardiomyocytes *in vivo*, and decreased the expression of markers of pathologic cardiac hypertrophy. In isolated adult cardiomyocytes after 2 weeks of POH and Ras-mutant gene transfer, N17-DN-Ras improved sarcomere shortening and calcium transients compared to Ras-Val12. Overall, DN-Ras promotes a more physiological form of hypertrophy, suggesting an interesting therapeutic target for pathological cardiac hypertrophy.

Keywords; heart failure, cardiac hypertrophy, ras oncogene, pathological hypertrophy, physiological hypertrophy.

INTRODUCTION

Small GTP binding-proteins are a superfamily of proteins acting as molecular switches between extracellular signals and molecular pathways [1, 2]. The Ras subfamily is the most important of the GTPases and includes three main homologous variants: H-Ras, K-Ras and N-Ras. The 3 genes are expressed ubiquitously with some variation in patterns of expression and function in developing and adult tissues [3, 4]**.**

H-Ras hyperactivity in the cardiomyocyte is associated with hypertrophy [2, 5]: *i)* In Costello's syndrome, patients with activating mutations of Ras develop hypertrophic cardiomyopathy with atrial tachycardia[6]. *ii)* Transgenic mice expressing the constitutively active mutant Ras-Val12 demonstrate ventricular hypertrophy similar to human hypertrophic cardiomyopathy[7]. *iii)* Mouse models of inducible cardiac overexpression of Ras-Val-12 have shown pathological features of cardiac hypertrophy[8]. Hypertrophy, deranged myofibril structure and impaired calcium transients is demonstrated in NRCM treated with Ras-Val-12[9].

On the other hand, Ras deficiency or Ras dominant negative mutants are associated with cardiac hypotrophy or anti-hypertrophic effects: *i)* K-Ras knock-out mice embryos die by day 15.5 of development, with very thin walls of cardiac ventricles as the likely cause of embryonic death [3]. *ii)* Thorburn et al. [10] showed that Ras-Ala15 (a negative interferent mutant of Ras) inhibits NRCM hypertrophy activated by phenylephrine (PE). Fuller et al. showed that N17-DNRas inhibits the hypertrophic effect of the active mutant of Src-Phe527 [11]. *iii)* Pracyk et al. [12] demonstrated the anti-hypertrophic effect of the N17-DN-Ras in neonatal cardiomyocytes at baseline, but not under stimulation by endotheline 1. *iv)* Recently, Nagalingam et al. [13] demonstrated the *in vitro* anti-hypertrophic effect of miR-378, a MicroRNA that negatively regulates Ras signaling in cardiac hypertrophy.

However, the study of the effects of Ras on cardiac hypertrophy is made difficult by the complex and poorly understood regulatory balance between proteins of the Ras

superfamily; moreover, there are several examples of paradoxical responses to Ras-dependent stimuli, such as Ras and Rap1 divergent actions [1, 14].

Ras mutants exert different actions at baseline or under ligand stimulation [12]. Duquesnes et al. [15] have shown that the ERK signaling pathway was down-regulated by DN-Ras in basal conditions but not under mechanical stimulation and Harris IS et al. [16] demonstrated apparently paradoxical actions of the Raf1-MAPkinase cascade. In mice expressing Ras-Val12 in the ventricles, the phenotype was variable and heterogeneous [5, 7, 17].

In this study, we hypothesized that the DN-Ras mutant N17 exerted an anti-hypertrophic effect *in vivo*, but we found a mixed agonist-antagonist action on the Ras pathway leading to cardiomyocyte hypertrophy or anti-hypertrophic effects, and the balance between the agonist and antagonist effects of N17-DN-Ras was stimulus-dependent. Furthermore, and beyond the hypertrophic response, we investigated the impact of N17-DN-Ras and active Ras-Val12 mutants on the pathologic character of cardiomyocyte hypertrophy. To that end, studies were conducted *in vitro* with and without pro-hypertrophic ligands, and *in vivo* in the setting of pressure-overload left ventricular (LV) hypertrophy (POH). To corroborate the results obtaiened by overexpressing dominant negative and active ras mutants, a set of experiments was performed using siRNA-H-Ras on NRCM.

MATERIALS AND METHODS

Recombinant adenovirus vectors.

All recombinant adenoviruses were constructed using a cytomegalovirus (CMV) promoter. Cells were infected with adenovirus at 50 to 100 MOI (multiplicities of infection) per cell. We used recombinant adenoviral vectors encoding two variants of the H-Ras gene: the dominant negative mutant S17N (Ad-DNRas) and the oncogenic active mutant G12V (Ad-Val12). The DN-Ras mutant of Ras (substitution of asparagine for serine at the 17^{th} amino-acid) is locked in its inactive form (Ras-GDP), due to a reduced affinity for GTP and preserved affinity for GDP [18]. The active mutant Ras Val12 (a substitution of glycine for valine, G12V, in the 12^{th} amino-acid) was used as a positive control for DN-Ras [5]. Ad-βGal, encoding β-galactosidase under CMV promoter followed by target gene-IRES-reporter gene (a green fluorescent protein (GFP)) construct translated as two independent proteins [19] was used as an additional control; Ad.NFAT-Luc virus, carrying the luciferase reporter gene controlled by NFAT- responsive promoter [20] was used to measure 4NFAT activation. Ad-VIVIT, encoding NFAT competing peptide VIVIT and GFP under CMV promoter[21, 22] was used as an additional control for NFAT-reporter experiments.

Isolation and culture of neonatal rat cardiomyocytes (NRCM). Spontaneously beating NRCM were isolated from 1 to 2-days-old Sprague-Dawley rat pups using the Worthington Neonatal Cardiomyocyte Isolation System (Worthington Biochemical Corp.) as previously described [23]. Cardiomyocytes were plated in12-well plates for 36h in serum-free medium then transduced with the recombinant adenoviruses (Ad-DNRas, Ad-Val12, or Ad-βGal) or no virus as control group.

For experiments using siRNA-H-Ras, NRCM were plated in 6-well plates in triplicates

and transfected with 50 nM Hras-siRNA (Santa Cruz Biotechnology) with RNAiMAX Transfection Reagent (Invitrogen) for 24 hours. Cells were then serum starved for 30 hours before they were stimulated with phenylephrine (1 uM) for an additional 24 hours. Cells were then harvested and homogenized for RNA and proteins preparation.

***Protein synthesis assay*.** Protein synthesis rate was measured using the [^{3}H]-Leucine incorporation assay as previously described [23]. Briefly, NRCM were transduced with the relevant adenovirus for 48h. Then, NRCM were stimulated for 7h with Phenylephrine (PE) (1 μM) or Angiotensin-II (1 μM) in the presence of [^{3}H]-Leucine. Protein synthesis was quantified by [^{3}H]-Leucine incorporation measured by scintillation counting (MicroBeta Trilux, Perkin Elmer).

In vitro and in vivo cardiomyocyte size measurement. Cell surface areas were measured on micrographs using the Image J software (NIH). At least 50 individual cells were analyzed for each experimental condition. For *in vivo* experiments, the size of cardiomyocytes was evaluated on cross sections using Wheat germ agglutinin (WGA) Alexa Fluor® 488 conjugate (Invitrogen).

In vitro beating analysis. We designed a protocol to keep NRCM beating for prolonged periods of time, and analyzed the influence of experimental genes on beating. NRCM were maintained with 2% serum in the medium instead of serum-free (0.1% serum) medium. After 24 hours with 2% serum, gene transfer was performed. Subsequent daily measurement of beating frequency was performed during 2 weeks. The beating frequency (beat/min) was counted in three different points of the well. The *in vitro* beating analysis was repeated three times, and with two wells per group each time.

Immunofluorescence. The sarcomeric structure of NRCM was analyzed by immunofluorescence with anti alpha-actinin (Sigma A2543), using standard protocol. Secondary antibody was a-rabbit IgG conjugated with Alexa 555 (Invitrogen). Slides were analyzed by confocal microscopy (Leica TCS-SP confocal microscopy).

***Quantitative Real time PCR*.** Total RNA was isolated with TRIzol reagent (Invitrogen). Expression of beta-Myosin-heavy-Chain (β-MHC), atrial natriuretic factor (ANF) and B-

type natriuretic peptide (BNP) mRNA in NRCM and LV tissue was quantified using real time RT-PCR (RT-PCR) analysis (7500 real-time PCR system, Applied Biosystems) performed according to standard procedures. Quantification of relative expression used the delta-delta-Ct approach. The following primers were used:

Rat-18S-F : 5'-GTTGGTTTTCGGAACTGAGGC
Rat-18S-R: 5'-GTCGGCATCGTTTATGGTCG

Rat ANF-F: 5'-ACC TGC TAG ACC ACC TGG AGG AG-3'
Rat ANF-R: 5'-CCT TGG CTG TTA TCT TCG GTA CCG-3'

Rat β-MHC-F: 5'-TTG GCA CGG ACT GCG TCA TC-3'
Rat β-MHC-R: 5'-GAG CCT CCA GAG TTT GCT GAA GGA-3'

Rat BNP-F: 5'-GCT GCT TTG GGC ACA AGA TAG-3'
Rat BNP-R: 5'-GGT CTT CCT ACA ACA ACT TCA-3'

Immunoblot analysis. Protein samples were prepared using a lysis buffer containing protease and phosphatase inhibitors (Roche), separated by SDS-PAGE and transferred on nitrocellulose membranes (Millipore). The membranes were blotted using standard protocol and revealed by chemiluminescence (Pierce). The following antibodies were used: p44/42 MAP kinase (Thr202/Tyr204) (Catalog No. 9101, Cell Signal Technology); p44/42 MAP kinase (Catalog No. 9102, Cell Signal Technology). Anti H-Ras proto-oncogene (Catalog No. SC-520 Santa Cruz Biotechnology), anti-pERK1/2, and anti-ERK1/2 (ref), Phospho-c-Raf (ser-259) (Catalog No. 9421 Cell Signaling Technology). Anti-Raf (Catalog No. 9422 Cell Signaling Technology) and anti-GAPDH: (Catalog No. 2118; Cell Signaling Technology). The densities of the immune-reactive bands were quantified using Image J software (NIH).

NFAT-promoter-Luciferase Reporter Assay. NRCM were infected with Ad.NFAT-LUC virus, carrying the luciferase reporter gene controlled by NFAT-responsive promoter [20], 48h after prior infection with Ras mutants and control adenoviruses. Ad-VIVIT, encoding the NFAT competing peptide VIVIT and GFP under CMV promoter, and FCS (10%) were used as negative and positive controls, respectively, for NFAT-reporter experiments. Luciferase activity was measured using the Luciferase Assay System (Promega) according to the manufacturer's instructions. Luciferase activity was normalized to total protein concentration for each sample as determined by Coomassie

Protein Assay Reagent (Pierce), and results were expressed as relative luciferase units per microgram of protein (RLU/μg).

In vivo adenoviral gene transfer in a rat pressure overload LV hypertrophy (POH) model. Animal care and procedures were performed with the approval of institutional animal care committees in accordance with the National Institute of Health's guide for the Care and Use of Laboratory Animals. Briefly, male rats (Sprague-Dawley, 250-300 g) were anesthetized with an intra-peritoneal injection of a combination of Ketamine (50-100 mg/Kg) and Xylazine (10 mg/Kg). The animal was intubated and ventilated. Midline thoracotomy was performed and the heart exposed. Cardiac gene delivery was performed with adenoviral vectors as previously reported [24-26]. A 24-gauge Angiocath was advanced from the apex of the LV to the aortic root. The aorta and pulmonary arteries were cross-clamped simultaneously distal to the site of the catheter, injecting the solution of adenovirus or control (saline solution), containing approximately 10^{10} plaque-forming units of the viruses, mixed with adenosine (50μl of a solution of adenosine 2mg/ml). The cross-clamp was maintained for 30 seconds. The blanching of the heart during the cross clamping indicated effective intracoronary injection. After the adenovirus delivery, rats were subjected to ascending aortic banding with a 0.58 mm (internal diameter) tantalum clip as previously described [24, 25]. A group of rats underwent a sham operation. The chest was vacuumed for removal of air and blood and closed in 3 layers. Four groups of animals were therefore studied *a)* Sham operated rats, *b)* POH with saline injection, *c)* POH with Ad.DN-Ras gene transfer. *d)* POH with Ad.RasV12 gene transfer.

Echocardiography and morphometric analysis. *In vivo* LV size and function was assessed by echocardiography at baseline (before surgery) and two weeks after surgery (prior to animal sacrifice). Animals were sedated with an intra-peritoneal injection of ketamine (50 mg/kg). Transthoracic two-dimensional (2D) and M-mode echocardiography was performed with a General Electric Vivid 7 system (General Electric, New York, NY) using an i13L 14 MHz transducer. M-mode echocardiography was performed on a mid-papillary-level LV short axis view as previously described [27]. After terminal echocardiography, rats were sacrificed and their hearts harvested. LV and right ventricle were separated and weighed. A ring of tissue from the LV mid-cavity was

embedded for histological analysis. The rest of the LV tissue was frozen for protein and RNA analysis. Selected hearts were used for cardiomyocyte isolation (see next paragraph).

Adult Rat Cardiomyocytes contractility and calcium transient assessment

Ventricular myocytes were isolated from rats two weeks after aortic constriction surgery and ras-mutant gene transfer via enzymatic dissociation, as previously described [28].

Cardiomyocytes were field-stimulated at a frequency of 1 Hz and were studied using the Ionoptic system, as previously described[28]. Sarcomeric shortening and relaxation was assessed using a video-based edge detection system (IonOptix). Calcium transients were obtained by loading cells with 0.5 μM fura2-AM (Invitrogen) and recording fluorescence measurements with a dual-excitation single-emission fluorescence photomultiplier system (IonOptix), as previously described[28].

Statistical analysis. *S*tatistical analysis used Student's T test or corresponding non-parametric tests, statistical significance threshold was $p<0.05$. All quantitative data are presented as mean ± standard error of the mean or standard deviation (SEM or SD).

RESULTS

1. Role of Ras in hypertrophic remodeling: a mixed agonist-antagonist effect of DN-Ras. We have examined the role of Ras in the hypertrophy-related signaling pathway using the neonatal rat cardiomyocytes (NRCM) and adenovirus encoding either constitutively active H-Ras (Ad-Val12) or dominant negative (Ad-DNRas). The efficacy of transduction was attested by GFP fluorescence (not shown); nearly 100% of cells were transduced. The expression of Ras mutants in NRCM was demonstrated by immunoblot analysis (**Fig.1A**). As shown in Fig.1A, transducing NRCM with a different range of MOI (10 to 500 MOI per cell) resulted in similar expression increase of Ras protein (**Fig.1A**).

Next, we analyzed the effect of different Ras mutants on hypertrophic growth of NRCM at baseline or with stimulation by phenylephrine (PE) (**Fig.1B**). At baseline, a significant increase of cardiomyocyte area was observed only in NRCM transduced with Ad-Val12 (**Fig.1B**). As expected, PE treatment (1μM, 48 h) resulted in a significant increase of cardiomyocytes size in non-infected or Ad-βGal transduced NRCM (**Fig.1B**). However in Ad-Val12-transduced group, PE treatment did not produce any additional effect on cell size, suggesting that Ras-Val12 activity was sufficient to achieve the maximal hypertrophic response. Although DN-Ras had no effect on cardiomyocytes size at baseline, it significantly inhibited PE-induced (1μM, 48h) hypertrophic growth of cardiomyocytes (**Fig. 1B)**.

Since NRCM hypertrophy is associated with an increase in protein synthesis [29], we assessed the effect of Ras mutants on Leucine incorporation (**Fig.1C**). As expected, Angiotensin-II (AT-II) and phenylephrine (PE) both increased Leucine incorporation compared with untreated conditions (no virus or β-Gal groups). Interestingly, DN-Ras has no significant effect on Leucine incorporation at baseline, while it prevented the increase in protein synthesis when cells were stimulated with AT-II or PE, in contrast with all other groups. As expected, Ras-Val12 increased Leucine incorporation at baseline, and further increased it in stimulated states (**Fig.1C**).

Then, in order to determine if Ras is involved in the control of hypertrophy-related signaling pathways, we analyzed the effect of different Ras proteins on the transcriptional activity of NFAT, the main activator of pathological cardiomyocyte hypertrophy [30]. As demonstrated in **Fig.1D**, NFAT-luciferase activity was increased in cardiomyocytes cultured in the presence of FCS (10%) and completely abolished in cardiomyocytes expressing the NFAT-competing peptide VIVIT, even in the presence of ATII, attesting to the specificity of the effect observed (**Fig.1D**). The transduction with control adenovirus (Ad-βGal) had no significant effect on basal NFAT-luciferase activity (**Fig.1D**), while the expression of Ras-Val12 was sufficient to induce a robust increase of NFAT transcriptional activity, even in the absence of other stimuli (**Fig.1D**), confirming previous observations[31]. As expected, ATII, which is known to induce an increase in intracellular Ca^{2+}[32], thereby activating the Ca^{2+}-dependent cytosolic factor NFAT[33] significantly increased NFAT-luciferase activity in Ad-βGal transduced cells, but could not increase this activity further in AdVal12 transduced cardiomyocytes, suggesting that RasVal12 maximally activated NFAT at the basal state (**Fig.1D**). Remarkably, DNRas has no effect on basal NFAT-luciferase activity but prevents the increase in this activity in the presence of ATII (**Fig.1D**), in agreement with its effect on protein synthesis (**Fig.1C**).

2. Activation of Ras adversely affects NRCM. Because hypertrophic remodeling is associated with alteration of cardiomyocyte structure and contractility, more precisely reduced sarcomere shortening and impaired contraction [34], we examined the effect of Ras mutants on spontaneous beating and sarcomere structure of NRCM (**Fig. 2**). NRCM were transduced with either Ad-Val12 or Ad-DNRas or Ad-βGal (control); spontaneously beating cells were monitored in culture for 14 days. In control cells (transduced with Ad-βGal), the rate of spontaneously beating cells was high (60 beats/min) until Day 5 after transduction. Then, the beating rate decreased dramatically to total cell beating arrest at Day 9. In the cells transduced with Ad-Val12, the beat rate dramatically decreased shortly after transduction to near arrest at Day 3 and was significantly lower than controls (**Fig. 2A**). By contrast, in the cultures transduced with Ad-DNRas, the beating rate decreased after transduction (Day 2) but remained

stable in the range of 20 to 40 beats/min until the end of experiment (Day 14). Thus, DN-Ras preserved NRCM beating, while Ras-Val12 abolished it, compared to control.

To determine whether the loss of beating was related to structural disorganization, we analyzed the effect of Ras mutants on α-actinin accumulation in Z-lines. It is known that i) α-actinin cross-links sarcomeric actin to Z-disc proteins; and ii) accumulation of α-actinin in the Z-disk depends on its phosphorylation [35] and iii) Ras-Val12 impairs sarcomeric structure[9].

Immunofluorescence with anti-α-actinin revealed a strong sarcomeric organization in control non-infected (not shown) or Ad-βGal infected cardiomyocytes (**Fig.2B**). However gene transfer of Ras-Val12 decreased α-actinin accumulation in Z-disks suggesting disorganization of sarcomere structure (**Fig.2B**). Interestingly, when NRCM were transduced with DN-Ras, the α-actinin accumulation to Z-disk was preserved (**Fig.2B**), suggesting normal sarcomeric organization. Thus, expression of constitutive active Ras (Ras-Val12) resulted in impaired cardiomyocyte beating supported by loss of α-actinin accumulation in Z-disk leading to sarcomeric disorganization.

3. Differential modulation of ERK and RAF phosphorylation by Ras mutants. The mechanism of action of DN-Ras was analyzed in the Ras-related pathway, specifically ERK phosphorylation modulation by Ras mutants when the NRCM were stimulated with AT-II or PE (1μM, 10 min) (**Fig. 3**). Both AT-II and PE significantly increased ERK phosphorylation in NRCM (**Fig.3A&B**). As expected, Ras-Val12 greatly increased ERK phosphorylation in the basal state and this activation is maintained under either stimulus (PE or AT-II) (**Fig. 3A**). By contrast, at basal state DN-Ras did not affect ERK phosphorylation (**Fig. 3B**). Moreover, DN-Ras expression prevented the increase of ERK phosphorylation under AT-II treatment (**Fig. 3B**). However, DN-Ras did not prevent ERK phosphorylation when activated by PE (**Fig. 3B**), indicating a stimulus-dependent antagonist activity of DN-Ras.

We also examined modulation of RAF phosphorylation under the same conditions. Indeed, RAF is currently considered as a first downstream signaling molecule

in RAS signaling cascade [36]. Surprisingly, AT-II and PE treatment only mildly increased RAF phosphorylation in NRCM (**Fig. 3C&D).** Along with this, Val-12 had a modest effect on RAF phosphorylation under basal conditions and did not affect Raf under PE or AT-II stimulation (**Fig. 3C).** Regarding the effect of DN-Ras on RAF, it mildly reduces RAF under AT-II and PE stimulation (**Fig. 3D**).

In summary, our *in vitro* data show that the expression of constitutive active Ras mutant is sufficient for induction of hypertrophic remodeling through NFAT activation. Dominant negative Ras has no effect on transcriptional activation of NFAT, but exert a mixed agonist-antagonist effect depending on the concurring hypertrophic stimulus.

4. Effect of siRNA-HRas on NRCM hypertrophy. Since the experiments involving dominant negative or activating Ras mutants required the over-expression of the mutant, and in order to dissect more deeply the Ras-dependence and the Ras-independence of the hypertrophic phenotype under study, we sought to corroborate our results with those of a silencing strategy using siRNA-HRas (**Fig. 4**). siRNA-HRas did not affect NRCM size at baseline but prevented the increase in NRCM size induced by phenylephrine (**Fig. 4A**). Interestingly, siRNA-HRas suppressed the baseline expression of the mRNA of β-MHC ANF and BNP in NRCM (**Fig. 4B-C-D**). The expression of the 3 genes markedly increased under phenylephrine stimulation, and this increase was blunted by the addition of siRNA-HRas (**Fig. 4B-C-D**). Nevertheless, phenylephrine retained a modest but significant stimulatory effect on the expression of β-MHC and ANF in the presence of siRNA-HRas (**Fig. 4B-C-D**), suggesting the parallel activity of Ras-dependent and Ras-independent mechanisms. A similar pattern was observed for the phosphorylation of ERK1, which was reduced by siRNA-HRas at baseline and stimulated by phenylephrine; (**Fig. 4E**). The phoshorylation of ERK1 was still increased by phenylephrine in the presence of siRNA-HRas, however, this increase was blunted (**Fig. 4E**). Phenylephrine and Ras siRNA did not significantly affect ERK2 phosphorylation (**Fig. 4E**).

I*n vivo,* the alteration of hemodynamic load results in the activation of multiple neurohormonal responses and intracellular signaling pathways involved in the regulation

of cardiac myocyte size and function. Thus, we hypothesized that *in vivo* modulation of intracellular signaling by Ras mutants results in differential adaptation of heart function to pressure overload. Therefore, we have analyzed the effect of Ras mutants on cardiac remodeling in a left ventricle (LV) pressure overload hypertrophy (POH) model.

5. Concurrent effect of Ras mutants and pressure-overload on early cardiac hypertrophy. Pressure-overload hypertrophy (POH) was induced in rats by aortic banding simultaneously with the gene transfer of Ras mutants. The animals were sacrificed 2 weeks after surgery. Effective gene transfer was verified by the increase in protein expression of Ras (**Fig. 5A**). Since there are no specific antibodies against Ras mutants, increased total Ras protein (H-Ras) expression indicated effective gene transfer (**Fig. 5A**).

5.1. DN-Ras prevented the pathologic hypertrophic remodeling of cardiomyocytes in the setting of POH. mRNA expression of hypertrophy-related genes was analyzed in LV tissue with POH with and without gene transfer of Ras mutants (**Fig. 5B&C**). As expected, POH increased the mRNA of ANF and β-MHC in LV tissue. Constitutively active Val12Ras further augmented the expression of hypertrophy-related genes in LV of POH animals (**Fig. 5B&C**). By contrast, DN-Ras prevented the increase of expression of both ANF and β-MHC in LV of POH animals suggesting a cardio-protective effect. We have measured the cross-sectional area of LV cardiomyocytes. As expected, POH significantly increased the size of cardiomyocytes in LV tissue (**Fig. 5D**). Expression of Val12Ras further enlarged the cardiomyocytes size as well as cardiomyocytes size variance in the setting of POH. Conversely, in DN-Ras transduced animals, the size of LV cardiomyocytes was similar to that in sham-operated animals (**Fig. 5D**), demonstrating the efficacy of inhibition of Ras signaling pathway by DN-Ras in early cardiac hypertrophy.

5.2. Both Ras-Val12 and DN-Ras increase LV/body weight ratio in the setting of POH. Two weeks after POH surgery, both Ras mutants appeared to exert a pro-hypertrophic effect as indicated by the ratio of LV/body weight, significantly higher than the AoB-saline control (**Fig. 6A, Table 1**). This finding is compatible with a partial agonist effect of DN-Ras on LV hypertrophy per se in the setting of POH. However, it

comes with a trend to a higher LV weight and to a lower body weight in DN-Ras-tranduced POH animals compared to saline control POH (**Table 1**). Ras mutants did not significantly affect the increase in LV wall thickness associated with POH (**Fig. 6B&C, Table 1**).

5.3. Ras-Val12 gene transfer increases LV systolic diameter and reduces LV fractional shortening compared to DN-Ras in the setting of pressure overload. LV diameters and fractional shortening were examined to test the hypothesis that, at similar levels of hypertrophy, Ras mutants had a different impact on LV function. As expected in a concentric LV hypertrophy pattern, LV diastolic diameters were reduced (compared to sham) in POH rats injected with saline and after DN-Ras gene transfer; this reduction was not significant after Ras-Val-12 gene transfer (**Fig. 6D, Table 1**). Likewise, LV systolic diameters were reduced in all 3 POH groups, however, LV systolic diameters were significantly higher with Ras-Val12 gene transfer than with either saline or DN-Ras (**Fig. 6E, Table 1**). Similarly, concentric POH resulted in an increase in LV fractional shortening; however, fractional shortening was lower in Ras-Val12 compared to DN-Ras and saline (**Fig. 6F, Table 1**). Altogether, these data corroborate the cardiotoxicity of Val12-Ras beyond hypertrophy, and a possible cardioprotective effect of DN-Ras consistent with what we observed in NRCM.

5.4. Ras-Val12 gene transfer alters cardiomyocytes contractility and calcium transients compared to DN-Ras in the setting of pressure overload.

Our findings in Figure 2 further demonstrate a known cardiotoxic effect of Ras-Val-12 on NRCM, in agreement with previous reports[9], and suggest a cardioprotective effect of DNRas. Moreover, both Ras mutants differentially affect contractile function and cardiac hypertrophy in POH (**Figure 6, Table 1**). Based on these results, we examined the effects of ras mutants on adult cardiomyocyte contractility and Ca^{2+} handling in the setting of POH. Ventricular myocytes were isolated from rats two weeks after simultaneous aortic banding surgery and gene transfer; subsequently, cardiomyocyte contractility and calcium transients were evaluated as described in the Methods section. **Figure 7A** shows recordings from representative control ventricular myocytes (sham operated) and POH myocytes infected with either AdVal12 or AdDNRas. Interestingly,

AdVal12 overexpression induced significant decreases in cell shortening compared to AdDNRas (4.83 ± 0.71 %, n=17 vs. 7.0 ± 0.66 %, n=11; P<0.05, **Fig. 7B**). Moreover, contraction half-time was shortened, indicating that contraction was accelerated in DNRas overexpressing cardiomyocytes (t1/2 on(s)L = 0.05 ± 0.003 μms for AdVal12, n=17 vs. 0.04 ± 0.001 μms for AdDNRas, n=11; P<0.05, **Fig. 7C**). Relaxation half-time was unchanged between mutants (t1/2 off (s)L): 0.1 ± 0.015 μms, n=17 vs. 0.09 ±0.014 μms, n=11; P=NS, **Fig. 7D**). These adult myocyte mechanical abnormalities are consistent with what has been observed in NRCM (**Fig. 2**) and alteration of ventricular function in vivo (**Fig. 6, Table 1**).

To evaluate whether the observed effect of Val12 on myocytes contractility is due to its effects on intracellular Ca^{2+} handling, cytoplasmic Ca^{2+} transients were determined in FURA-2 loaded ventricular myocytes. Ca^{2+} transients following POH and AdVal12 overexpression were reduced (19.46 ± 1.45 %, n=17) compared to either control (30.89 ± 3.19 %, n=17; P<0.01) or AdDNRas-transduced myocytes (22.96 ± 2.01%, n=13; P<0.01) (**Fig. 7E and 7F**). There was no effect on the rising half-time of the calcium transient (**Fig. 7G);** however, the half-time of calcium transient decay was accelerated only in the DNRas group (**Fig. 7H)**.

DISCUSSION

Central role of Ras in physiologic and/or pathologic cardiomyocyte hypertrophy.

Pathologic cardiomyocyte hypertrophy is the result of a complex interaction between signaling pathways leading to a manifold response beyond myocyte growth [5, 30]. This interaction likely results in an equilibrium, which is in turn displaced by the addition of Ras mutants, variably affecting hypertrophy and some of its aspects. Cardiomyocyte hypertrophy is not limited to an increase in cell size but is rather a multiform process involving transcriptional events, new protein synthesis, and changes in the myofilament organization [12, 30].

Previous reports indeed suggest that Ras mutants have mixed agonist and antagonist effects on cardiac hypertrophy which are modulated by concurring hypertrophic stimuli: Gottshall et al. [7] mentioned signifiant variability of phenotype among Ras-Val-12 transgenic mice; one explanation for this variability within and between studies may reside in the fine balance on which the Ras system operates and the easy displacement of the Ras equilibrium.

Here, we demonstrated a cardio-protective effect of N17-DN-Ras beyond its variable antihypertrophic effect using *in vitro* and *in vivo* gene transfer studies. *In vitro*, DN-Ras maintains NRCM beating and enhances Z line structure, is antihypertrophic on NRCM activated by PE, and inhibits NFAT. *In vivo*, DN-Ras decreased the expression levels of β-MHC and ANF in hypertrophied hearts and reduced the cross-sectional area of cardiac myocytes. Furthermore, DN-Ras enhances contractility and ameliorates Ca^{2+} transient in cardiomyocytes in the setting of POH, in comparison to the detrimental effects of Ras-Val12. In a previous study, Ras-Val12 mutants impaired calcium transients in NRCM[9].

Taken together, our data show that the Ras signaling cascade can be involved in physiological and/or pathological adaptations of cardiomyocyte strucutre and function to altered haemodynamics, depending on stimuli combination (**Fig. 8**). Physiological adaptation can be achieved through modulation of the RAS/RAF/ERK signaling pathway; whereas pathological remodeling requires the activation of the transcription factor NFAT [37, 38]. Indeed, the expression of a constitutively active Ras mutant

induced transcriptional activation of NFAT, sarcomeric disorganization and cardiac dysfunction.

Dominant negative Ras inhibits the agonist-induced transcriptional activation of NFAT, but allows ERK phosphorylation under particular conditions. Furthermore, the mixed agonist-antagonist effect of DN-Ras is dependent on the concurring hypertrophic stimuli.

Our study of the effect of Ras mutants on cardiomyocyte hypertrophy shows for the first time that a known DN-Ras mutant (Ras N17) can allow physiological hypertrophy to occur, while it is antihypertrophic under classical ligand stimulation, favoring a mixed agonist-antagonist response rather than a mere competitive antagonism. This evidence highlights the difference within signaling pathways activated during pathological and physiological remodeling. The mixed agonist and antagonist actions of DN-Ras, as well as the agonist actions of active Val-12 Ras are stimulus-dependent. This behavior suggests that Ras does not have a simple switch on-off function but a highly complex role of modulation, depending on the stimulus, as highlighted by the varied responses of cardiomyocytes to ras mutants in our experiments. Besides, we studied the differential action of Ras mutants beyond mere hypertrophy, affecting sarcomeric organization *in vitro*, the pathologic character of LV hypertrophy and ensuing LV and cardiomyocyte function in the setting of POH *in vivo*.

Pathologic prohypertrophic effect of active Ras-Val12.

i. Cardio-toxicity of Val12-Ras vitro. Here we have demonstrated that Ras-Val12 gene transfer to NRCM caused sarcomeric disorganization and inhibited the beating of cardiomyocytes, consistent with the finding of Ho et al[9]. Unlike us, Thorburn et al. [10] found that Ras-Val12 increased the organization of sarcomeres similarly to phenylephrine. Differences in the promoter used may explain the different results, since, in our study, Ras-Val-12 was overexpressed through a CMV promoter, while in the study by Thorburn et al. Ras-Val-12 was overexpressed using its native Ras promoter [10].

We suggest that cardio-toxicity of Val12-Ras could be related to the involvement of active Ras in the transcriptional activation of the pro-hypertrophic transcription factor

NFAT. Indeed, as demonstrated here, the expression of constitutive active Ras mutant was sufficient to activate NFAT in the absence of others stimuli. In relation with this, Ras-Val12 abolished NRCM beating within a few days after gene transfer, whereas, DN-Ras maintained their beating for a longer time than controls. This result, together with the enhancement of the sarcomeric structure by DN-Ras, strongly suggests not only a pro-hypertrophic effect of Ras-Val12 but also a cardiotoxic one, while DN-Ras shows cardio-protective properties despite a mixed-agonist-antagonist effect on hypertrophy.

ii. Effects of Val12-Ras in vivo in the setting of POH. Previously, Hunter J. et al. [17] have reported that Ras-Val12 induced left ventricular hypertrophy with myocyte disarray and diastolic dysfunction in transgenic mice; however, echocardiography was not performed in the latter study, therefore, LV geometry was not determined. Another study by the same group [7] in echocardiography-selected transgenic mice demonstrates concentric LV hypertrophy with increased wall thickness, intraventricular obstruction and reduced fractional shortening in Ras-Val12 mice. In contrast, our study of the added effect of Ras-Val12 gene transfer on POH by ascending aortic banding demonstrates a more eccentric hypertrophy associated with a significant increase in LV end-systolic diameter and a trend to reduce LV wall thickness along with the previously demonstrated [7] reduced fractional shortening. In addition, data from our study revealed that POH ventricular myocytes transduced with Ras-Val12 exhibited depressed sarcomeric shortening and depressed calcium transients compared to healthy cardiomyocytes and POH cardiomyocytes overexpressing DN-Ras, confirming the cardiotoxic effect of Ras-Val12 in vivo.

DN-Ras as a mixed agonist-antagonist of cardiomyocyte hypertrophy.

i. Comparison of DN-Ras N17 with other DN-Ras mutants. Our study shows that active and dominant-negative Ras mutants differentially affect the different aspects of hypertrophy. Ras has been shown to modulate NFAT activation in NRCM, with induction by Val-12-Ras and inhibition of agonist-induced NFAT activation by N17-DNRas [31]. In our experiments, Val-12 Ras activated NFAT without concurring stimulation, whereas DN-Ras had no effect on NFAT activity in basal conditions, but

prevented the ATII-induced increase of NFAT-luciferase activity, confirming previous observations [31].

The effects observed with dominant negatives Ras mutants depend of the type of mutant. We used an N17 mutant employed also by other studies [12, 15, 39] whereas several studies employed the Ala15-Ras inhibitor [10, 40]. The inhibitory action of DN-Ras-N17 is due to a reduced affinity for GTP and a normal affinity for GDP [18]. Interestingly, it has been noted that Ras mutants with reduced affinity for both GDP and GTP did not inhibit growth [18], suggesting that Ras mutations affecting GTP binding are more than a simple on-off switch and favoring our mixed agonist-antagonist hypothesis, balanced by the molecular context. Indeed, the actions of N17-DNRas are mediated by interaction with Ras-guanine nucleotide exchange factors (Ras-GEF) [5].

ii. Differential Modulation of ERK and Raf by DN-Ras. The analysis of the classical Ras pathway showed that in NRCM stimulated by AT-II, DN-Ras blocked Raf and ERK phosphorylation; but when the NRCM were stimulated with PE, DN-Ras down-regulated Raf phosphorylation but did not block ERK phosphorylation, supporting a stimulus-dependent modulation of ERK by DNRas and PE. This observation is consistent with Lei et al. who found that Phenylephrine activates ERK by trans-activating EGFR and FGFR (Epidermal and Fibroblast Growth Factor Receptors) independent of the Ras/Raf/ERK pathway [41], and is also consistent with the data from Duquesnes N et al. [15]. However these data contrast with the study of Zou et al.[39]. There are clear methodological differences between the two studies. For example, in the study by Zou et al.[39], pharmacologic inhibition of the farnesylation of Ras was used, and N17-DNras was expressed using plasmids with 3-5% transfection efficiency, while our study used adenoviral vectors. Moreover, the study by Zou et al.[39] measured the phosphorylating activity of ERK and Raf-1 rather than the phosphorylation measured by us. Our data with AT-II and PE are of interest since they reveal a more potent activation of ERK than of Raf-1, and the Ras-dependence of the activation of these targets by AT-II, but not by PE, for ERK. Thus, the blocking effect of DN-Ras can be overridden by alternative signaling pathways.

This fine regulation of DN-Ras that modulates ERK phosphorylation under AT-II but not under PE is a very important observation illustrating the mixed, apparently

paradoxical, agonist-antagonist effect of DN-Ras found *in vitro* and *in vivo*. On the other hand, active Ras-Val12 phosphorylated ERK strongly, but it increased phospho-Raf only slightly. DN-Ras did not block ERK and Raf as consistently as expected. A likely explanation is that the DN-Ras N17 mutant has a negative phenotype, but it is not a negative null type mutant: DN-Ras decreases the affinity of Ras for GTP from 1×10^{-8} to $1 \times 10^{-6.5}$ [18], maintaining a relatively low but steady activation of Ras, permitted by the binding to GTP that activates Ras.

iii. Ras inhibition by siRNA-H-Ras as an alternative approach to N17-DN-Ras

Considering that the results obtained with DN-Ras were mitigated by the overexpression of a protein which was not a negative null mutant, we complemented our experiments by the study of the effects of siRNA-H-Ras transfection on NRCM. To our knowledge, this is the first study to use that approach. As shown in **Fig. 4**, siRNA-H-Ras inhibited PE-induced NRCM hypertrophy and blunted the PE-induced expression of hypertrophic markers as well as the PE-induced phosphorylation of ERK1. Interestingly, siRNA-H-Ras reduced the baseline expression of molecular markers of hypertrophy and the baseline phoshorylation of ERK1 (**Fig. 4 B-E).** Moreover, PE had a significant stimulatory effect on β-MHC and ANF expression despite the presence of siRNA-H-Ras (**Fig. 4 B,C)** along with the ability to induce the phoshorylation of ERK1 (**Fig. 4 E)** suggesting an additive effect of Ras-dependent and Ras-independent mechanisms, especially for the agonist-induced phosphorylation of ERK.

iv. The complex effects of N17-DNRas on rat POH. Here, in contrast with a previous study by Pracyk JB et al. [12], we have demonstrated that N17-DN-Ras transduction preserved the sarcomeric organization and beating in cultured NRCM, suggesting a cardioprotective effect of DNRas *in vitro*. In line with these findings on NRCM, adult ventricular myocytes subjected to simultaneous POH and transduction with DNRas exhibited sarcomere shortening similar to control and even accelerated contraction. Calcium transients in DNRas transduced cardiomyocytes did not differ significantly from control transients, while calcium transient decay was significantly accelerated.

When superimposed on POH, DN-Ras did not affect LV geometry nor did it inhibit LV hypertrophy; it indeed seemed to favor hypertrophy as assessed by LV/body weight ratio

(Fig. 6A, Table 1). In addition, we have demonstrated that DN-Ras prevented the hypertrophic growth of cardiomyocytes in vitro and the POH-induced increase in cardiomyocyte cross-sectional area in vivo. There are a few possible explanations to the contrast between the data on cardiomyocyte cross-sectional area in vivo and LV weight/body weight. Body weights of rats at baseline were similar between groups **(Table 1)**. At two weeks after surgery, body weight tended to be lower in DN-Ras than in saline or sham groups, but was significantly lower in Val-12 Ras, likely reflecting blunted weight gain associated with adenoviral injection **(Table 1)**. Taken together, a trend to a higher LV weight for DN-Ras vs saline and a trend to a lower body weight could explain the marginal increase in LV weight/body weight ratio for DN-Ras vs saline **(Fig. 6A, Table 1)**. We attribute body weight differences to the attenuation of weight gain by adenoviral infection.

Nonetheless, the analysis of the regulatory mechanisms of Ras *in vivo* showed that N17-DN-Ras suppressed the induction of β-MHC and ANF by POH, while the latter remained increased with the transfection of Val-12-Ras, although not exacerbated by it. This lack of *in vivo* anti-hypertrophic effect of DN-Ras in POH can be explained mainly by the presence of Ras-independent pathways. Figure 7 summarizes the intracellular signaling pathways modulated by Ras in cardiomyocytes. The Ras-independent pathways were suggested by *in vitro* experiments by Pracyk et al. [12] and others[39, 41]. Pressure-overload induces the release of the prohypertrophic ligands endotheline, angiotensin and phenylephrine [16]. These ligands are prohypertrophic through Ras-dependent and Ras-independent pathways [14, 40]. Besides, Duquesnes et al. have shown that N17-DN-Ras plasmid transfection inhibited ERK activation in NRCM at baseline but not under stretch[15]. Finally, our in vitro experiments of ERK and Raf phosphorylation show that DN-Ras can block ERK phosphorylation when the cardiac cells are stimulated by AT-II but not by PE. These Ras-independent pathways, together with the previously reported stimulus-dependent modulation of cardiomyocyte hypertrophy by DNRas, provide explanations to the lack of antihypertrophic effect of DN-Ras in the *in vivo* experiments involving POH. In addition, and as mentioned earlier, parallel Ras-dependent and Ras-independent mechanisms appear to be at work in the PE-induced phosphorylation of ERK1 **(Fig. 4E).**

Limitations

Our study suffers limitations of conceptual and methodological nature. We used classical designs (NRCM, POH) to study a protein previously shown to affect cardiomyocyte hypertrophy; however, we went on to evaluate the functional consequences of Ras modulation in the setting of hypertrophy. Measurable POH after 2 weeks is indeed observed in this study and in previous studies[26, 42]. Nevertheless, significant myocardial dysfunction following POH is best evaluated in longer studies, where significant ventricular dilatation and transition to heart failure can be observed. Such a study would require the use of adeno-associated virus for gene expression, while in the present study, we used adenoviral vectors and were limited by the 2 weeks duration of expression these vectors allow in vivo[43].

CONCLUSIONS.

The present study is, to our knowledge, the first one to study Ras modulation in pressure-overload hypertrophy, and, in that setting, it showed DN-Ras to be cardio-protective, although it was not anti-hypertrophic. This lack of anti-hypertrophic effect can be explained by mixed agonist-antagonist effects of DN-Ras that are stimulus-dependent, and by the complexity of certain stimuli, such as pressure-overload. Furthermore, this cardio-protective effect of DN-Ras has some similarities with physiologic hypertrophy, especially the lower expression level of β-MHC and ANF, along with the improved sarcomere shortening and calcium-handling patterns. It is consistent with our finding of improved sarcomeric morphology and preserved *in vitro* beating of neonatal cardiomyocytes. All these characteristics of DN-Ras make Ras an interesting therapeutic target in pathological cardiac hypertrophy.

Acknowledgments. The adenovirus with DN-Ras was a kind gift from Dr. Mladen Golubic (Center for Integrative Medicine, Cleveland Clinic, Cleveland, Ohio), while the oncogenic mutant of Ras-Val12 was a gift of Dr. Mario I Romero-Ortega (Regenerative Neurobiology Lab, The University of Texas, Arlington, TX). We thank Susan Kraner and Christopher M. Norris (Sanders-Brown Center on Aging, Lexington, KY-USA) for providing AdVIVIT. Special thanks to Dr. Juan Ramón Fabregat for his support and advice.

Disclosure. The authors have no conflict of interest to disclose.

Sources of Funding. This study was supported in part by NIH RO1 HL083156, HL080498, HL093183, and P20HL100396 (RJH); Association Française contre les Myopathies (AFM 16442; LL, RJH); NIHNHLBI T32HL007824 (ERC).

None of the funding sources was involved in study design; in the collection, analysis and interpretation of data; in the writing of the report; and in the decision to submit the article for publication.

Table 1: Echocardiographic and morphometric analysis of the left ventricle (LV) after pressure overload hypertrophy (POH) and H-Ras mutants gene transfer (a) LV and body weight (BW) (b) LV diastolic wall thickness (c) LV cavity diameter and fractional shortening. SD, standard deviation

(a) LV and body weight (BW)

group		BW(g)	BW(g)	LVweight(mg)	LVweight/ BW(mg/g)
timepoint		**baseline**	**2 weeks**	**2 weeks**	**2 weeks**
Sham	**mean**	289.00	391.23	869.78	2.20
	SD	30.39	33.60	84.86	0.25
	n	7	13	9	9
AAB+Saline	**mean**	285.00	382.67	1120.50	2.93
	SD	29.31	30.74	142.52	0.34
	n	3	6	6	6
	p vs. Sham	0.85	0.6	0.0009	0.0003
AAB+DN-Ras	**mean**	274.83	367.10	1221.43	3.27
	SD	39.03	32.41	42.06	0.16
	n	6	10	7	7
	p vs. Sham	0.47	0.098	<0.0001	<0.0001
	p vs. AAB+Saline	0.71	0.36	0.0999	0.0401
AAB+Ras-Val12	**mean**	270.40	336.30	1108.44	3.25
	SD	28.70	33.31	151.85	0.25
	n	10	10	9	9
	p vs. Sham	0.22	0.0008	0.0008	<0.0001
	p vs. AAB+Saline	0.46	0.015	0.89	0.054
	p vs. AAB+DN-Ras	0.80	0.0505	0.0780	0.91

(b) LV diastolic wall thickness

group		LV anterosceptal wall thickness in diastole (cm)	LV anterosceptal wall thickness in diastole (cm)	LV posterior wall thickness in diastole (cm)	LV posterior wall thickness in diastole (cm)
timepoint		**baseline**	**2 weeks**	**baseline**	**2 weeks**
Sham	**mean**	0.19	0.20	0.20	0.20
	SD	0.02	0.02	0.03	0.03
	n	13	13	13	13
AAB+Saline	**mean**	0.19	0.26	0.20	0.27
	SD	0.01	0.02	0.02	0.02
	n	6	7	6	7
	p vs. Sham	0.76	<0.0001	0.74	<0.0001
AAB+DN-Ras	**mean**	0.19	0.27	0.20	0.28
	SD	0.02	0.02	0.03	0.02
	n	10	10	10	10
	p vs. Sham	0.98	<0.0001	0.79	<0.0001
	p vs. AAB+Saline	0.76	0.97	0.92	0.446
AAB+Ras-Val12	**mean**	0.17	0.25	0.18	0.26
	SD	0.01	0.03	0.02	0.03

	n	10	10	10	10
	p vs. Sham	0.033	0.0004	0.086	0.0001
	p vs. AAB+Saline	0.0046	0.19	0.031	0.306
	p vs. AAB+DN-Ras	0.028	0.12	0.039	0.10

(c) LV cavity diameter and fractional shortening

group		**LV diastolic diameter (cm)**	**LV diastolic diameter (cm)**	**LV systolic diameter (cm)**	**LV systolic diameter (cm)**	**LV Fractional shortening (%)**	**LV Fractional shortening (%)**
timepoint		**baseline**	**2 weeks**	**baseline**	**2 weeks**	**baseline**	**2 weeks**
Sham	**mean**	0.58	0.66	0.20	0.24	67	64
	SD	0.06	0.07	0.07	0.07	10	7
	n	13	13	13	13	13	13
AAB+ Saline	**mean**	0.61	0.55	0.21	0.10	65	81
	SD	0.05	0.09	0.05	0.02	5	3
	n	6	7	6	7	6	7
	p vs. Sham	0.28	0.008	0.71	0.0001	0.79	<0.0001
AAB+ DN-Ras	**mean**	0.58	0.60	0.18	0.12	69	81
	SD	0.05	0.06	0.06	0.03	8	5
	n	10	10	10	10	10	10
	p vs. Sham	0.93	0.041	0.46	<0.0001	0.50	<0.0001
	p vs. AAB+Saline	0.25	0.19	0.24	0.29	0.33	0.89

AAB+ Ras-Val12	**mean**	0.59	0.62	0.19	0.15	68	76
	SD	0.07	0.05	0.06	0.03	7	4
	n	10	10	10	10	10	10
	p vs. Sham	0.64	0.12	0.87	0.0013	0.76	0.003
	p vs. AAB+Saline	0.62	0.06	0.55	0.0018	0.48	0.0146
	p vs. AAB+DN-Ras	0.69	0.44	0.52	0.013	0.65	0.02

FIGURE CAPTIONS

Figure 1. Modulation of hypertrophic remodeling of NCRM by Ras mutants.

A. Expression of Ras proteins in transduced NRCM. Representative immunoblot showing expression of H-Ras protein in NRCM transduced for 48 h with relevant adenoviruses at multiple ranges of MOI (Multiplicity of Infection). Expression of H-Ras expression was low to undetectable in non-transduced or β-gal transduced NRCM at this time of exposure.

B. Modulation of cell size by Ras-mutants and Phenylephrine (PE) in NRCM. Relative cardiomyocyte size (cell area) of control or transduced with indicated adenovirus NRCM. Cells were cultured for 48 h with PE (1 μM) or vehicle. Area values were normalized to area of control (non transduced) NRCM. Number of cardiomyocytes measured for each condition was ~ 60 from three independent experiments. *** $p<0.001$.

C. Modulation of protein synthesis ([^{3}H]-Leucine incorporation) by Angiotensin-II (AT-II), Phenylephrine (PE) and Ras-mutants in NRCM. Bar-graph showing [^{3}H]-Leucine by NRCM under different conditions. NRCM were transduced with Ad-βGal, Ad-DNRas or Ad-RasVal12 for 48h, and stimulated for 7 h with Phenylephrine (PE) (1μM) or Angiotensin-II (1μM) in the presence of [^{3}H]-Leucine. The data are presented as normalized mean ± standard error (SEM) of three independent experiments performed in triplicata. * $p<0.05$; *** $p<0.001$

D. Ras controls the major prohypertrophic transcription factor NFAT. Promoter-reporter assay of NFAT transcriptional activity. Twenty-four hours after transduction with Ad-NFAT-Luc, NRCM were infected with indicated Ad-βGal, Ad-Val12, Ad-DNRas or Ad-VIVIT for 48 h. Ad-VIVIT, encoding NFAT competing peptide VIVIT and GFP under CMV promoter and FCS (10%) were used as negative and positive controls, respectively. Data (mean values ± SEM of at least three independent experiments) are expressed in relative luciferase units (RLU) as a percentage of value in Ad-βGal infected cells. ***** $p < 0.05$; ******* $p < 0.001$.

Figure 2. Activation of Ras leads to sarcomeric disorganization and impaired beating in NRCM.

A. Monitoring of spontaneous beating frequency in NRCM transduced with Ad-βGal,~~;~~ Ad-Ras-Val12 or Ad-DNRas during 14 days. Cells were transduced at Day 0. n=4 cells per time point and per condition. Both Ras-Val12 and DN-Ras were compared to Beta-Gal with *p<0.05, **p<0.01 and ***p<0.001 and DN-Ras was compared to Ras-Val12 with $p<0.05, $$p<0.01 and $$$p<0.001 **B, C et D.** Analysis of sarcomeric structure of NRCM transduced with Ad-βGal **(B)**; Ad-Ras-Val12 **(C)** or Ad-DNRas **(D)** for 3 days. Left panel: immunofluorescence with α-Actinin showing the position of the Z-band. Right panel: profile showing the optical density (gray plot) along the white line. Images show the representative pattern observed in at least 60% of the cells. Magnification 40X.

Figure 3. Modulation of ERK (A and B) and RAF (C and D) phosphorylation by Ras mutants under AT-II or PE stimulation. Upper panel: typical immunoblot showing relative levels of phosphorylation of ERK and Raf proteins at the basal conditions or under stimulation by AT-II (1µM, 10 min) or PE (1µM, 10 min). Lower panel: bar-graph showing the relative expression of the same proteins. Data (mean values ± SEM of at least three independent experiments) are expressed as a percentage of value in control condition (non infected, non treated). ***** $p < 0.05$.

Figure 4. Impact of siRNA-H-Ras treatment on phenylephrine-induced hypertrophy in NRCM

A. NRCM size after treatment with siRNA-H-Ras and/or PE. N=84 to 122 cells per conditions were measured. **B, C and D.** Normalized expression of the mRNA of βMHC, ANF and BNP; N=2-3 per condition, t-test performed on the delta-delta-Ct. **E.** Western blot and band quantification of the phoshorylation of ERK1 and ERK2; N=2 bands per condition. *p<0.05, **p<0.01 and ***p<0.001

<u>Figure 5.</u> Impact of Ras gene transfer on left ventricular pressure-overload hypertrophy.

A. Representative immunoblot (left panel) and quantification (right panel) showing H-Ras expression in LV of control animals or animals transduced with indicated virus.
n=2 per group, *p< 0.05.

B&C. Box plots of the RT-PCR analysis of the relative mRNA expression of hyperthrophic markers (ANF (**B**) and beta-MHC (**C**)) in LV tissue from control animals or POH animals transduced with indicated virus. All the groups were normalized *versus* the levels of 18S mRNA. N=2-3 animals per group. ***** $p < 0.05$; ******$p < 0.01$ for t-test performed on the delta-delta-Ct

D. Analysis of LV cardiomyocyte cross-sectional area in control (sham operated) and POH animals transduced with indicated adenovirus. Left panel: Germ agglutinin staining. Right panel: Bar graph representing the mean cardiomyocytes cross-sectional area in 3 sham- and 4 POH-operated animals. 250 individual measurements from 5 sections were performed for each animal. ******* $p < 0.001$ (Non-parametric Kruskal-Wallis test followed by Dunn's Multiple Comparison Test).

<u>Figure 6.</u> Morphometric and Echocardiographic analysis of rat LV in the setting of combined POH and Ras mutant gene transfer.

7-13 animals per group were analyzed (see **Table 1** for details).

***** $p < 0.05$; ******$p < 0.01$; ******* $p < 0.001$

A. Morphometric analysis. LV weight/body weight is increased as a result of POH, and further increased by gene transfer of either DN-Ras or Val12-Ras. AoB, ascending aortic banding.

B&C. LV anteroseptal (**B**) and posterior (**C**) wall thickness were increased significantly in all POH groups. No significant difference was related to Ras mutants. **D**. LV diastolic diameter at 2 weeks was reduced by AoB with saline or DNRas, but failed to decrease with Ras-Val12.

E. LV systolic diameter was reduced in all POH groups; it was significantly increased in the Val12-Ras group compared to other POH.

F. LV fractional shortening increased in POH as a result of concentric LV hypertrophy; it was significantly reduced with Val12-Ras gene transfer compared to other POH.

Figure 7. Effects of Ras mutants on adult rat cardiomyocyte contractility and Ca^{2+} transients in the setting of POH

A, Representative tarcings of sarcomere shortening from control myocytes and myocytes subjected to 2 weeks of POH and simultaneously transduced with Ad.Val12 or Ad.DNRas *in vivo*. **B**, Sarcomere shortening, as a % of resting cell length. **C**, Time to Half Contraction (t1/2 on (s) L). **D**, Time to Half Relaxation (t1/2 off (s) L). L – length of cardiomyocytes; **E**, representative Ca^{2+} transient tracings. **F**, Ca^{2+} transient, diastolic ratio. **G**, Calcium transient rising half-time (t1/2 on (s) R). **H,** Calcium transient decay half-time (t1/2 off (s) R). R – FURA-2 340/380 ratio. Average parameters of cardiomyocyte contraction were determined (control: n=9; Ad.Val12, n=17; AdDNRas, n=11 cells); average of calcium transient parameters were determined (control: n=17; Ad.Val12, n=23; AdDNRas, n=13 cells) *P<0.05, **P<0.01.

Figure 8. Simplified schema showing the intracellular signaling pathways modulated by Ras in cardiomyocytes (adapted from Diana E. Jaalouk & Jan Lammerding,[44]).
At the level of cardiomyocytes, hemodynamic alterations and neurohormonal ligands can be sensed through a diverse group of membrane-anchored mechanosensors including ion channels, cell-membrane-spanning G-protein-coupled receptors, and growth-factor receptors. This mechanical sensing is then converted to biochemical signals by triggering the multi-step activation of downstream partners in an array of signaling cascades in the cytoplasm. The highlights of such cascades include the three modules of the mitogen-activated protein kinase (MAPK) family underscored by the activation of Ras, the PLC-related cascade leading to the alteration of Ca^{2+} signaling and PI3K signaling cascade required for the induction of of hypertrophic remodeling. The convergence of these pathways results in the activation of specific transcription factors including the nuclear factor of activated T cells (NFAT), involved in hypertrophic remodeling. Singular activation of ERK signaling (through RAF or directly by GPCR) seems to support adaptive physiological remodeling. Ultimately, the net sum of gene-expression reprogramming in

cardiomyocytes dictates the structural and functional response of a cell to pressure overload.

Abbreviations: SR – sarcoplasmic reticulum; DAG – diacylglycerol; IP3 - inositol 1,4,5-triphosphate; PLC – phospholipase C; PI3K - phosphatidyl-inositol 3-kinase; AKT - protein kinase B; GSK - Glycogen synthase kinase-3beta; CaN – calcineurine, protein phosphatase 2B; NFAT - nuclear factor of activated T cells; MEKK - mitogen-activated protein kinase; ERK - extracellular signal–regulated kinase.

References:

[1] S.C. Jeyaraj, N.T. Unger, M.A. Chotani, Rap1 GTPases: an emerging role in the cardiovasculature, Life sciences, 88 (2011) 645-652.

[2] F. Lezoualc'h, M. Metrich, I. Hmitou, N. Duquesnes, E. Morel, Small GTP-binding proteins and their regulators in cardiac hypertrophy, Journal of molecular and cellular cardiology, 44 (2008) 623-632.

[3] K. Koera, K. Nakamura, K. Nakao, J. Miyoshi, K. Toyoshima, T. Hatta, H. Otani, A. Aiba, M. Katsuki, K-ras is essential for the development of the mouse embryo, Oncogene, 15 (1997) 1151-1159.

[4] L.M. Esteban, C. Vicario-Abejon, P. Fernandez-Salguero, A. Fernandez-Medarde, N. Swaminathan, K. Yienger, E. Lopez, M. Malumbres, R. McKay, J.M. Ward, A. Pellicer, E. Santos, Targeted genomic disruption of H-ras and N-ras, individually or in combination, reveals the dispensability of both loci for mouse growth and development, Molecular and cellular biology, 21 (2001) 1444-1452.

[5] A. Clerk, P.H. Sugden, Small guanine nucleotide-binding proteins and myocardial hypertrophy, Circulation research, 86 (2000) 1019-1023.

[6] A.L. Schulz, B. Albrecht, C. Arici, I. van der Burgt, A. Buske, G. Gillessen-Kaesbach, R. Heller, D. Horn, C.A. Hubner, G.C. Korenke, R. Konig, W. Kress, G. Kruger, P. Meinecke, J. Mucke, B. Plecko, E. Rossier, A. Schinzel, A. Schulze, E. Seemanova, H. Seidel, S. Spranger, B. Tuysuz, S. Uhrig, D. Wieczorek, K. Kutsche, M. Zenker, Mutation and phenotypic spectrum in patients with cardio-facio-cutaneous and Costello syndrome, Clinical genetics, 73 (2008) 62-70.

[7] K.R. Gottshall, J.J. Hunter, N. Tanaka, N. Dalton, K.D. Becker, J. Ross, Jr., K.R. Chien, Ras-dependent pathways induce obstructive hypertrophy in echo-selected transgenic mice, Proceedings of the National Academy of Sciences of the United States of America, 94 (1997) 4710-4715.

[8] B.R. Wei, P.L. Martin, S.B. Hoover, E. Spehalski, M. Kumar, M.J. Hoenerhoff, J. Rozenberg, C. Vinson, R.M. Simpson, Capacity for resolution of Ras-MAPK-initiated early pathogenic myocardial hypertrophy modeled in mice, Comparative medicine, 61 (2011) 109-118.

[9] P.D. Ho, D.K. Zechner, H. He, W.H. Dillmann, C.C. Glembotski, P.M. McDonough, The Raf-MEK-ERK cascade represents a common pathway for alteration of intracellular calcium by Ras and protein kinase C in cardiac myocytes, The Journal of biological chemistry, 273 (1998) 21730-21735.

[10] A. Thorburn, J. Thorburn, S.Y. Chen, S. Powers, H.E. Shubeita, J.R. Feramisco, K.R. Chien, HRas-dependent pathways can activate morphological and genetic markers of cardiac muscle cell hypertrophy, The Journal of biological chemistry, 268 (1993) 2244-2249.

[11] S.J. Fuller, J. Gillespie-Brown, P.H. Sugden, Oncogenic src, raf, and ras stimulate a hypertrophic pattern of gene expression and increase cell size in neonatal rat ventricular myocytes, The Journal of biological chemistry, 273 (1998) 18146-18152.

[12] J.B. Pracyk, D.D. Hegland, K. Tanaka, Effect of a dominant negative ras on myocardial hypertrophy by using adenoviral-mediated gene transfer, Surgery, 122 (1997) 404-410; discussion 410-401.

[13] R.S. Nagalingam, N.R. Sundaresan, M.P. Gupta, D.L. Geenen, R.J. Solaro, M. Gupta, A cardiac-enriched microRNA, miR-378, blocks cardiac hypertrophy by targeting Ras signaling, The Journal of biological chemistry, 288 (2013) 11216-11232.

[14] G.X. Zhang, S. Kimura, K. Murao, X. Yu, K. Obata, H. Matsuyoshi, M. Takaki, Effects of angiotensin type I receptor blockade on the cardiac Raf/MEK/ERK cascade activated via adrenergic receptors, Journal of pharmacological sciences, 113 (2010) 224-233.

[15] N. Duquesnes, F. Vincent, E. Morel, F. Lezoualc'h, B. Crozatier, The EGF receptor activates ERK but not JNK Ras-dependently in basal conditions but ERK and JNK activation pathways are predominantly Ras-independent during cardiomyocyte stretch, The international journal of biochemistry & cell biology, 41 (2009) 1173-1181.

[16] I.S. Harris, S. Zhang, I. Treskov, A. Kovacs, C. Weinheimer, A.J. Muslin, Raf-1 kinase is required for cardiac hypertrophy and cardiomyocyte survival in response to pressure overload, Circulation, 110 (2004) 718-723.

[17] J.J. Hunter, N. Tanaka, H.A. Rockman, J. Ross, Jr., K.R. Chien, Ventricular expression of a MLC-2v-ras fusion gene induces cardiac hypertrophy and selective diastolic dysfunction in transgenic mice, The Journal of biological chemistry, 270 (1995) 23173-23178.

[18] L.A. Feig, G.M. Cooper, Inhibition of NIH 3T3 cell proliferation by a mutant ras protein with preferential affinity for GDP, Molecular and cellular biology, 8 (1988) 3235-3243.

[19] F. del Monte, S.E. Harding, U. Schmidt, T. Matsui, Z.B. Kang, G.W. Dec, J.K. Gwathmey, A. Rosenzweig, R.J. Hajjar, Restoration of contractile function in isolated

cardiomyocytes from failing human hearts by gene transfer of SERCA2a, Circulation, 100 (1999) 2308-2311.

[20] E. Merlet, L. Lipskaia, A. Marchand, L. Hadri, N. Mougenot, F. Atassi, L. Liang, S.N. Hatem, R.J. Hajjar, A.M. Lompre, A calcium-sensitive promoter construct for gene therapy, Gene therapy, 20 (2013) 248-254.

[21] J. Aramburu, F. Garcia-Cozar, A. Raghavan, H. Okamura, A. Rao, P.G. Hogan, Selective inhibition of NFAT activation by a peptide spanning the calcineurin targeting site of NFAT, Molecular cell, 1 (1998) 627-637.

[22] J. Aramburu, M.B. Yaffe, C. Lopez-Rodriguez, L.C. Cantley, P.G. Hogan, A. Rao, Affinity-driven peptide selection of an NFAT inhibitor more selective than cyclosporin A, Science, 285 (1999) 2129-2133.

[23] D. Lebeche, Kang, Z. B., Hajjar, R., Candesartan abrogates G proteincoupled receptors agonist-induced MAPK activation and cardiac myocyte hypertrophy., J Renin. Angio. Aldosterone, 2001 (2001) S154-S161.

[24] R.J. Hajjar, U. Schmidt, T. Matsui, J.L. Guerrero, K.H. Lee, J.K. Gwathmey, G.W. Dec, M.J. Semigran, A. Rosenzweig, Modulation of ventricular function through gene transfer in vivo, Proceedings of the National Academy of Sciences of the United States of America, 95 (1998) 5251-5256.

[25] F. del Monte, R.J. Hajjar, Efficient viral gene transfer to rodent hearts in vivo, Methods in molecular biology, 219 (2003) 179-193.

[26] G. Choukroun, R. Hajjar, S. Fry, F. del Monte, S. Haq, J.L. Guerrero, M. Picard, A. Rosenzweig, T. Force, Regulation of cardiac hypertrophy in vivo by the stress-activated protein kinases/c-Jun NH(2)-terminal kinases, The Journal of clinical investigation, 104 (1999) 391-398.

[27] R.M. Lang, M. Bierig, R.B. Devereux, F.A. Flachskampf, E. Foster, P.A. Pellikka, M.H. Picard, M.J. Roman, J. Seward, J.S. Shanewise, S.D. Solomon, K.T. Spencer, M.S. Sutton, W.J. Stewart, G. Chamber Quantification Writing, G. American Society of Echocardiography's, C. Standards, E. European Association of, Recommendations for chamber quantification: a report from the American Society of Echocardiography's Guidelines and Standards Committee and the Chamber Quantification Writing Group, developed in conjunction with the European Association of Echocardiography, a branch of the European Society of Cardiology, Journal of the American Society of Echocardiography : official publication of the American Society of Echocardiography, 18 (2005) 1440-1463.

[28] M. Kim, J.K. Oh, S. Sakata, I. Liang, W. Park, R.J. Hajjar, D. Lebeche, Role of resistin in cardiac contractility and hypertrophy, Journal of molecular and cellular cardiology, 45 (2008) 270-280.

[29] S. Kang, E.R. Chemaly, R.J. Hajjar, D. Lebeche, Resistin promotes cardiac hypertrophy via the AMP-activated protein kinase/mammalian target of rapamycin (AMPK/mTOR) and c-Jun N-terminal kinase/insulin receptor substrate 1 (JNK/IRS1) pathways, The Journal of biological chemistry, 286 (2011) 18465-18473.

[30] I. Kehat, J.D. Molkentin, Molecular pathways underlying cardiac remodeling during pathophysiological stimulation, Circulation, 122 (2010) 2727-2735.

[31] M. Ichida, T. Finkel, Ras regulates NFAT3 activity in cardiac myocytes, The Journal of biological chemistry, 276 (2001) 3524-3530.

[32] J. Sadoshima, Z. Qiu, J.P. Morgan, S. Izumo, Angiotensin II and other hypertrophic stimuli mediated by G protein-coupled receptors activate tyrosine kinase, mitogen-

activated protein kinase, and 90-kD S6 kinase in cardiac myocytes. The critical role of Ca(2+)-dependent signaling, Circulation research, 76 (1995) 1-15.

[33] N. Koitabashi, T. Aiba, G.G. Hesketh, J. Rowell, M. Zhang, E. Takimoto, G.F. Tomaselli, D.A. Kass, Cyclic GMP/PKG-dependent inhibition of TRPC6 channel activity and expression negatively regulates cardiomyocyte NFAT activation Novel mechanism of cardiac stress modulation by PDE5 inhibition, Journal of molecular and cellular cardiology, 48 (2010) 713-724.

[34] G.t. Cooper, Cytoskeletal networks and the regulation of cardiac contractility: microtubules, hypertrophy, and cardiac dysfunction, American journal of physiology. Heart and circulatory physiology, 291 (2006) H1003-1014.

[35] B. Sjoblom, A. Salmazo, K. Djinovic-Carugo, Alpha-actinin structure and regulation, Cellular and molecular life sciences : CMLS, 65 (2008) 2688-2701.

[36] F. Chang, L.S. Steelman, J.T. Lee, J.G. Shelton, P.M. Navolanic, W.L. Blalock, R.A. Franklin, J.A. McCubrey, Signal transduction mediated by the Ras/Raf/MEK/ERK pathway from cytokine receptors to transcription factors: potential targeting for therapeutic intervention, Leukemia, 17 (2003) 1263-1293.

[37] J.D. Molkentin, Calcineurin and beyond: cardiac hypertrophic signaling, Circulation research, 87 (2000) 731-738.

[38] J.D. Molkentin, Calcineurin-NFAT signaling regulates the cardiac hypertrophic response in coordination with the MAPKs, Cardiovascular research, 63 (2004) 467-475.

[39] Y. Zou, I. Komuro, T. Yamazaki, R. Aikawa, S. Kudoh, I. Shiojima, Y. Hiroi, T. Mizuno, Y. Yazaki, Protein kinase C, but not tyrosine kinases or Ras, plays a critical role in angiotensin II-induced activation of Raf-1 kinase and extracellular signal-regulated

protein kinases in cardiac myocytes, The Journal of biological chemistry, 271 (1996) 33592-33597.

[40] V.J. LaMorte, J. Thorburn, D. Absher, A. Spiegel, J.H. Brown, K.R. Chien, J.R. Feramisco, K.U. Knowlton, Gq- and ras-dependent pathways mediate hypertrophy of neonatal rat ventricular myocytes following alpha 1-adrenergic stimulation, The Journal of biological chemistry, 269 (1994) 13490-13496.

[41] B. Lei, D.A. Schwinn, D.P. Morris, Stimulation of alpha1a adrenergic receptors induces cellular proliferation or antiproliferative hypertrophy dependent solely on agonist concentration, PloS one, 8 (2013) e72430.

[42] H. Jin, E.R. Chemaly, A. Lee, C. Kho, L. Hadri, R.J. Hajjar, F.G. Akar, Mechanoelectrical remodeling and arrhythmias during progression of hypertrophy, FASEB journal : official publication of the Federation of American Societies for Experimental Biology, 24 (2010) 451-463.

[43] A.M. Lompre, L. Hadri, E. Merlet, Z. Keuylian, N. Mougenot, I. Karakikes, J. Chen, F. Atassi, A. Marchand, R. Blaise, I. Limon, S.W. McPhee, R.J. Samulski, R.J. Hajjar, L. Lipskaia, Efficient transduction of vascular smooth muscle cells with a translational AAV2.5 vector: a new perspective for in-stent restenosis gene therapy, Gene therapy, 20 (2013) 901-912.

[44] D.E. Jaalouk, J. Lammerding, Mechanotransduction gone awry, Nature reviews. Molecular cell biology, 10 (2009) 63-73.

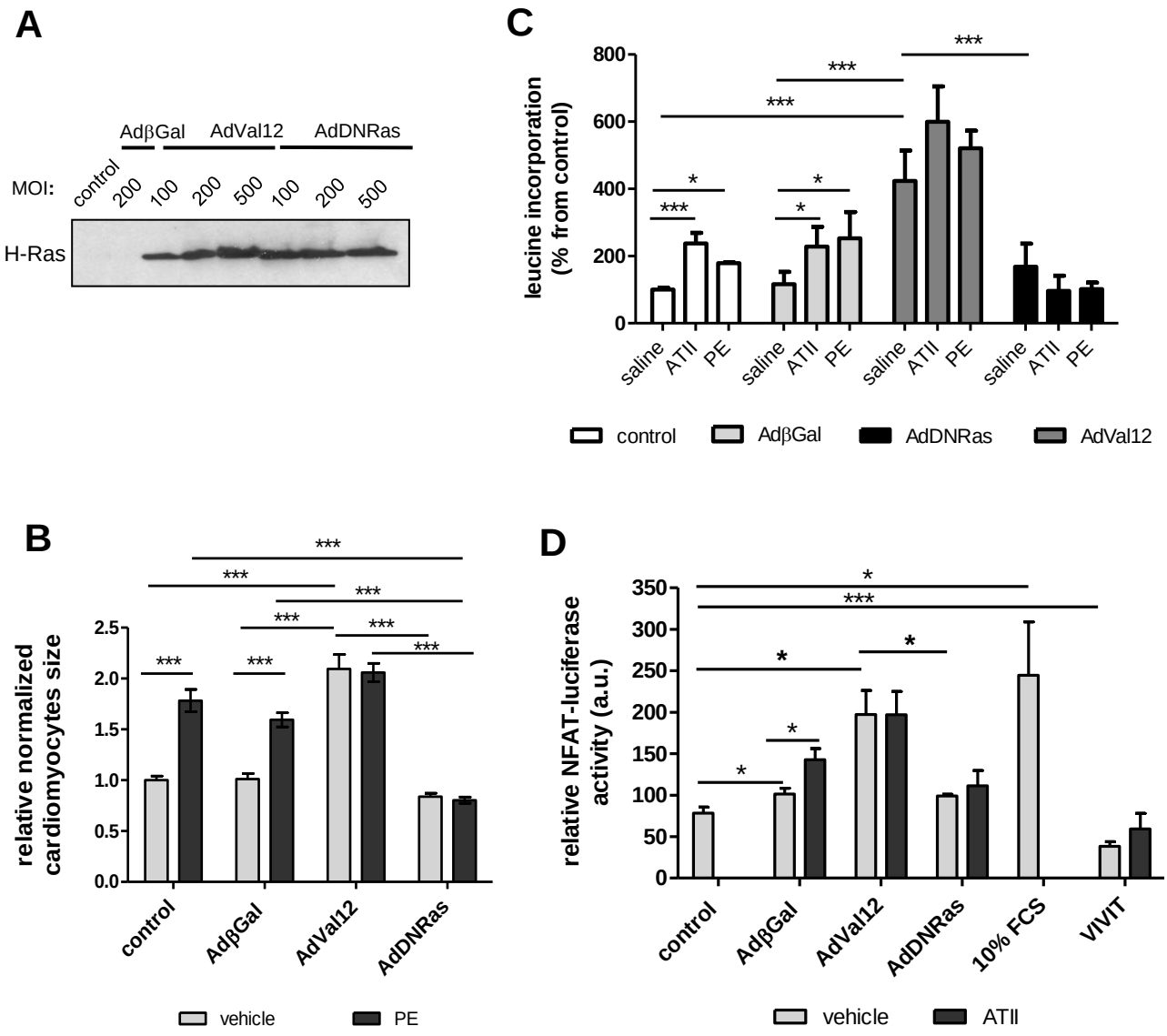
A
AdβGal
AdVal12
AdDNRas
MOI:
control
200
100
200
500
100
200
500
H-Ras
C
leucine incorporation (% from control)
800
600
400
200
0
***
*
saline
ATII
PE
control
AdβGal
AdDNRas
AdVal12
B
relative normalized cardiomyocytes size
2.5
2.0
1.5
1.0
0.5
0.0
control
AdβGal
AdVal12
AdDNRas
vehicle
PE
D
relative NFAT-luciferase activity (a.u.)
350
300
250
200
150
100
50
0
10% FCS
VIVIT
vehicle
ATII

Figure 1.

A

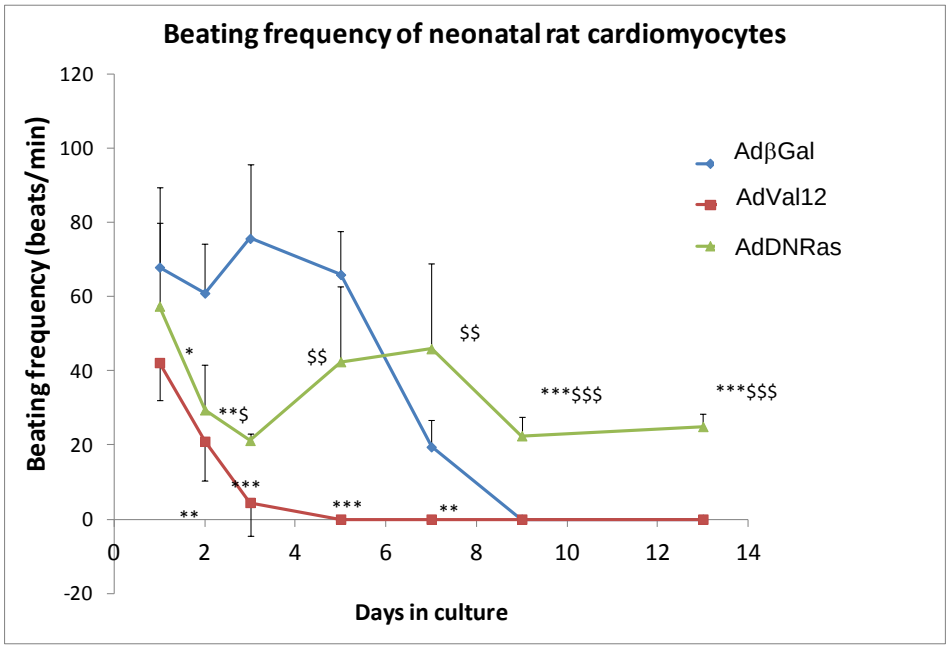

B

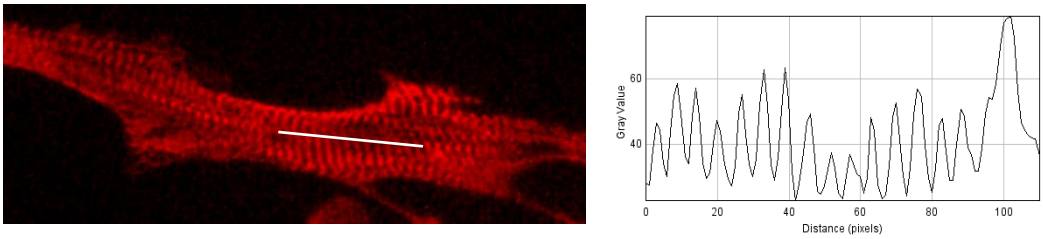

C

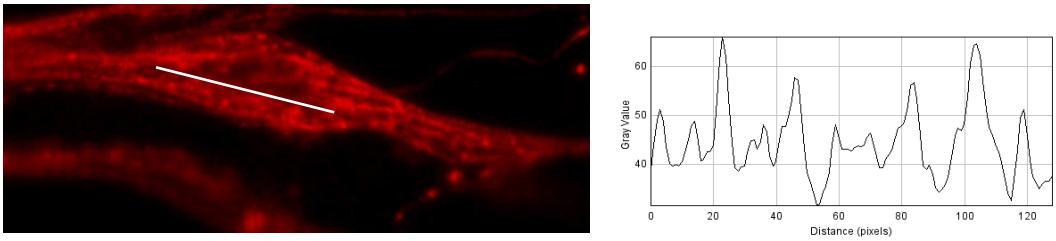

D

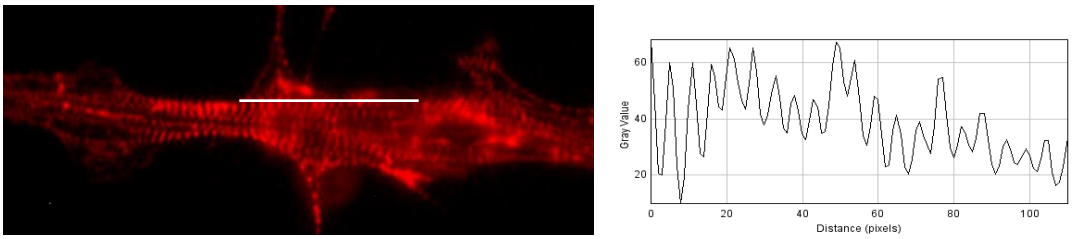

Figure 2.

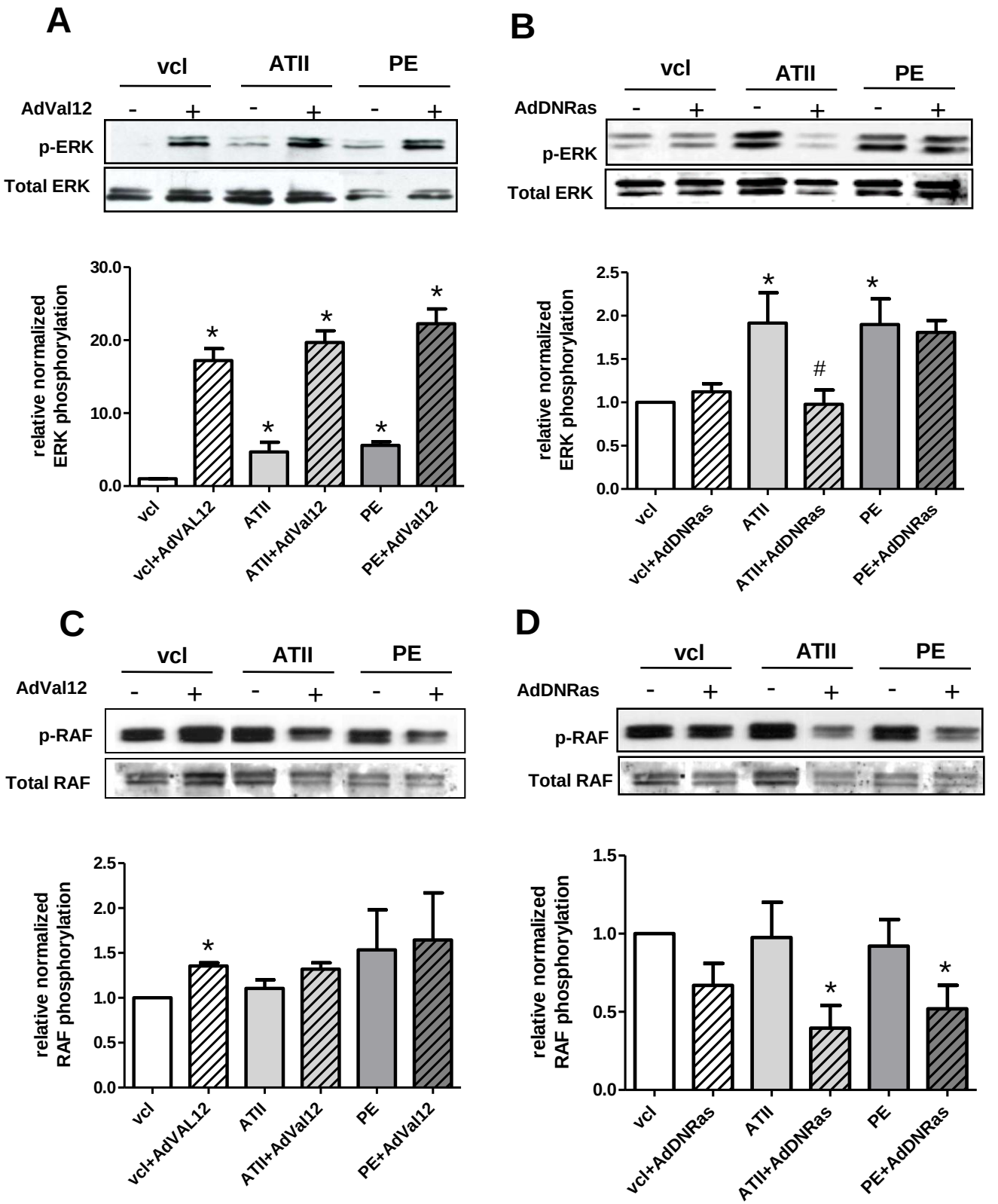
A
vcl
ATII
PE
AdVal12
- + - + - +
p-ERK
Total ERK
relative normalized ERK phosphorylation
30.0
20.0
10.0
0.0
vcl
vcl+AdVAL12
ATII
ATII+AdVal12
PE
PE+AdVal12
B
vcl
ATII
PE
AdDNRas
- + - + - +
p-ERK
Total ERK
relative normalized ERK phosphorylation
2.5
2.0
1.5
1.0
0.5
0.0
#
vcl
vcl+AdDNRas
ATII
ATII+AdDNRas
PE
PE+AdDNRas
C
vcl
ATII
PE
AdVal12
- + - + - +
p-RAF
Total RAF
relative normalized RAF phosphorylation
2.5
2.0
1.5
1.0
0.5
0.0
vcl
vcl+AdVAL12
ATII
ATII+AdVal12
PE
PE+AdVal12
D
vcl
ATII
PE
AdDNRas
- + - + - +
p-RAF
Total RAF
relative normalized RAF phosphorylation
1.5
1.0
0.5
0.0
vcl
vcl+AdDNRas
ATII
ATII+AdDNRas
PE
PE+AdDNRas

Figure 3.

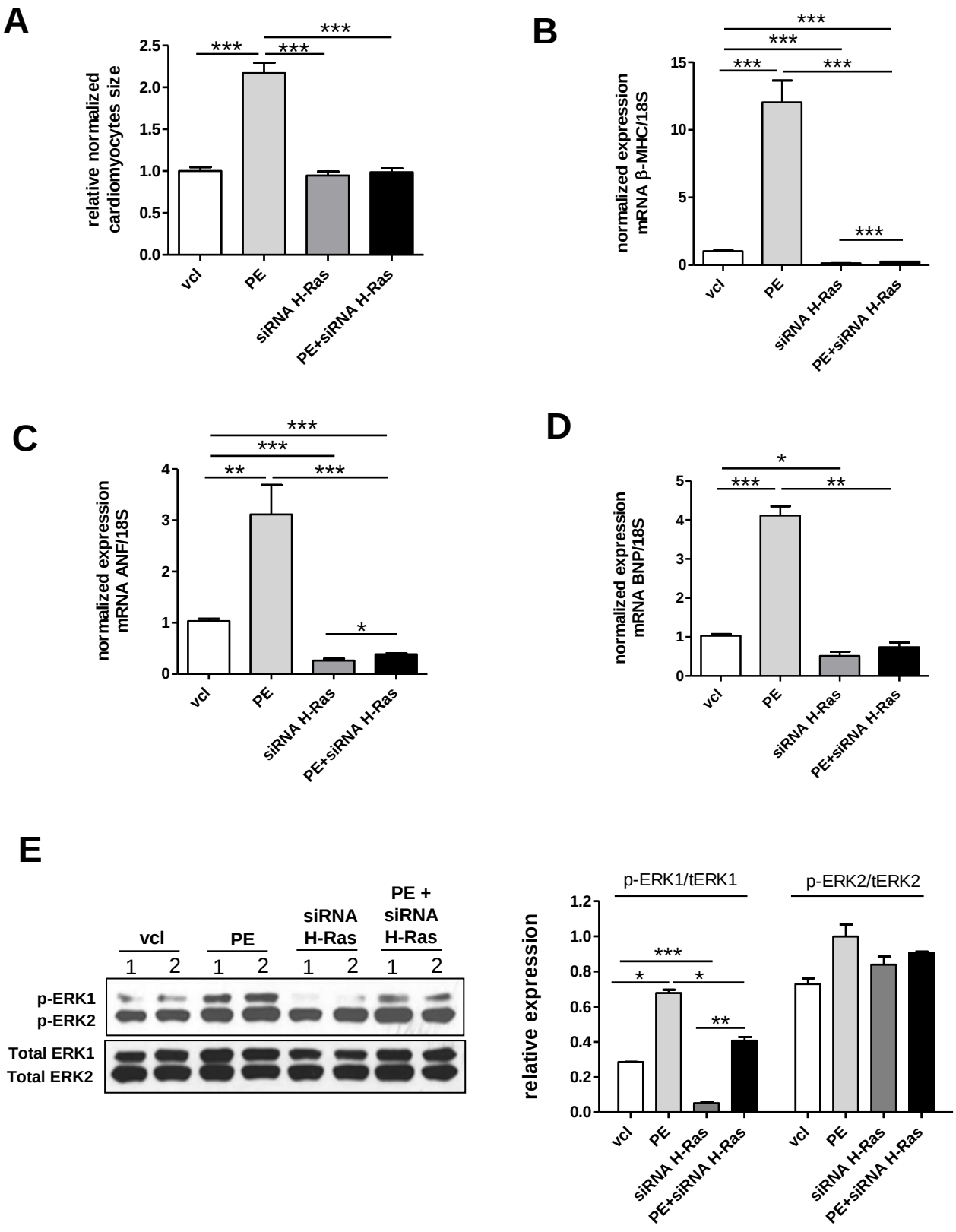
A
relative normalized cardiomyocytes size
2.5
2.0
1.5
1.0
0.5
0.0
***
***
***
vcl
PE
siRNA H-Ras
PE+siRNA H-Ras
B
normalized expression mRNA β-MHC/18S
15
10
5
0
***
***
***
***
***
vcl
PE
siRNA H-Ras
PE+siRNA H-Ras
C
normalized expression mRNA ANF/18S
4
3
2
1
0
***
***
**
***
*
vcl
PE
siRNA H-Ras
PE+siRNA H-Ras
D
normalized expression mRNA BNP/18S
5
4
3
2
1
0
*
***
**
vcl
PE
siRNA H-Ras
PE+siRNA H-Ras
E
vcl
PE
siRNA H-Ras
PE + siRNA H-Ras
1 2 1 2 1 2 1 2
p-ERK1
p-ERK2
Total ERK1
Total ERK2
p-ERK1/tERK1
p-ERK2/tERK2
relative expression
1.2
1.0
0.8
0.6
0.4
0.2
0.0
***
*
*
**
vcl
PE
siRNA H-Ras
PE+siRNA H-Ras
vcl
PE
siRNA H-Ras
PE+siRNA H-Ras

Figure 4.

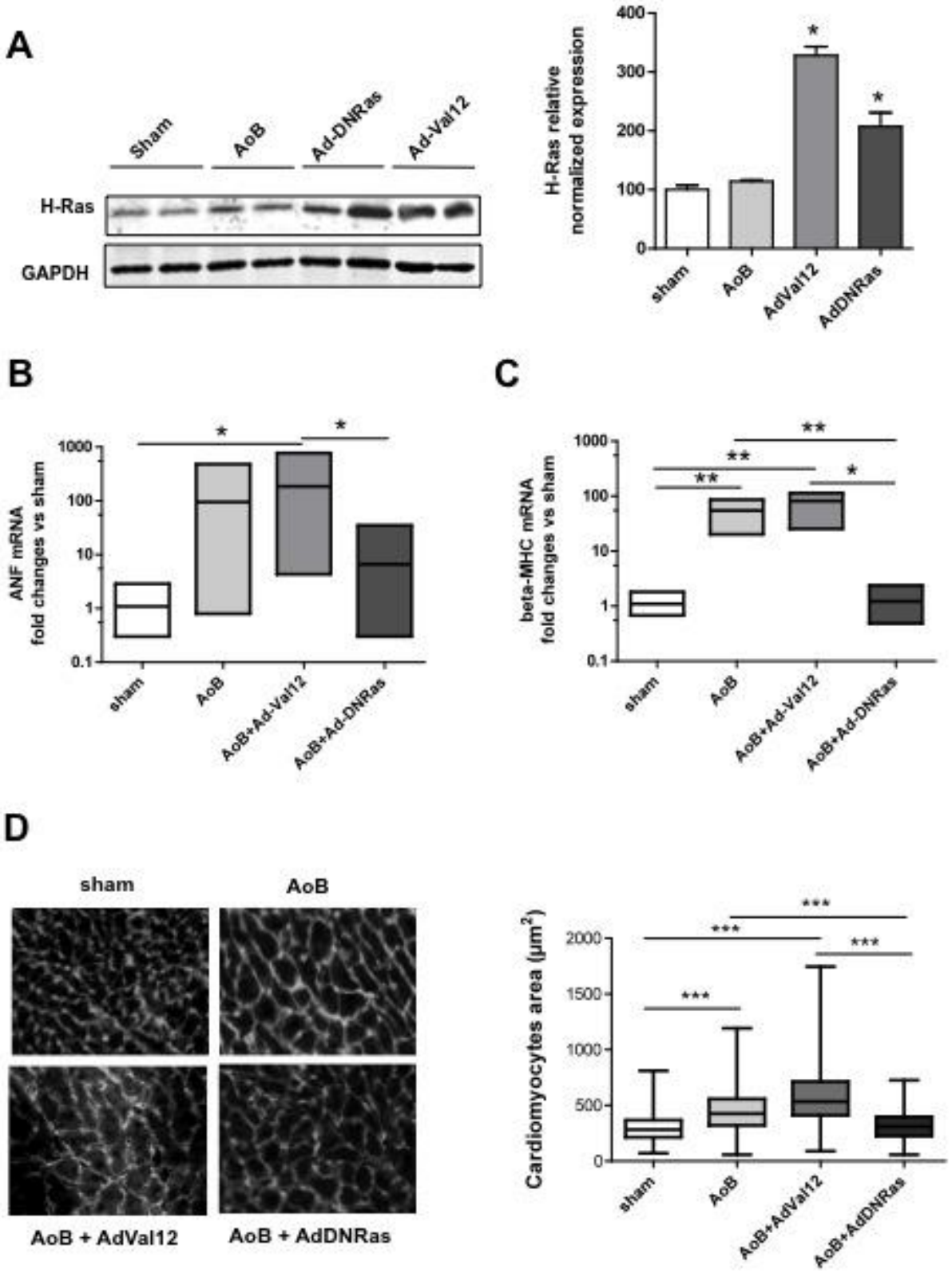
A
Sham
AoB
Ad-DNRas
Ad-Val12
H-Ras
GAPDH
H-Ras relative normalized expression
400
300
200
100
0
*
*
sham
AoB
AdVal12
AdDNRas
B
ANF mRNA fold changes vs sham
1000
100
10
1
0.1
*
*
sham
AoB
AoB+Ad-Val12
AoB+Ad-DNRas
C
beta-MHC mRNA fold changes vs sham
1000
100
10
1
0.1
**
**
**
*
sham
AoB
AoB+Ad-Val12
AoB+Ad-DNRas
D
sham
AoB
AoB + AdVal12
AoB + AdDNRas
Cardiomyocytes area (μm²)
2000
1500
1000
500
0
***
***
***
***
sham
AoB
AoB+AdVal12
AoB+AdDNRas

Figure 5.

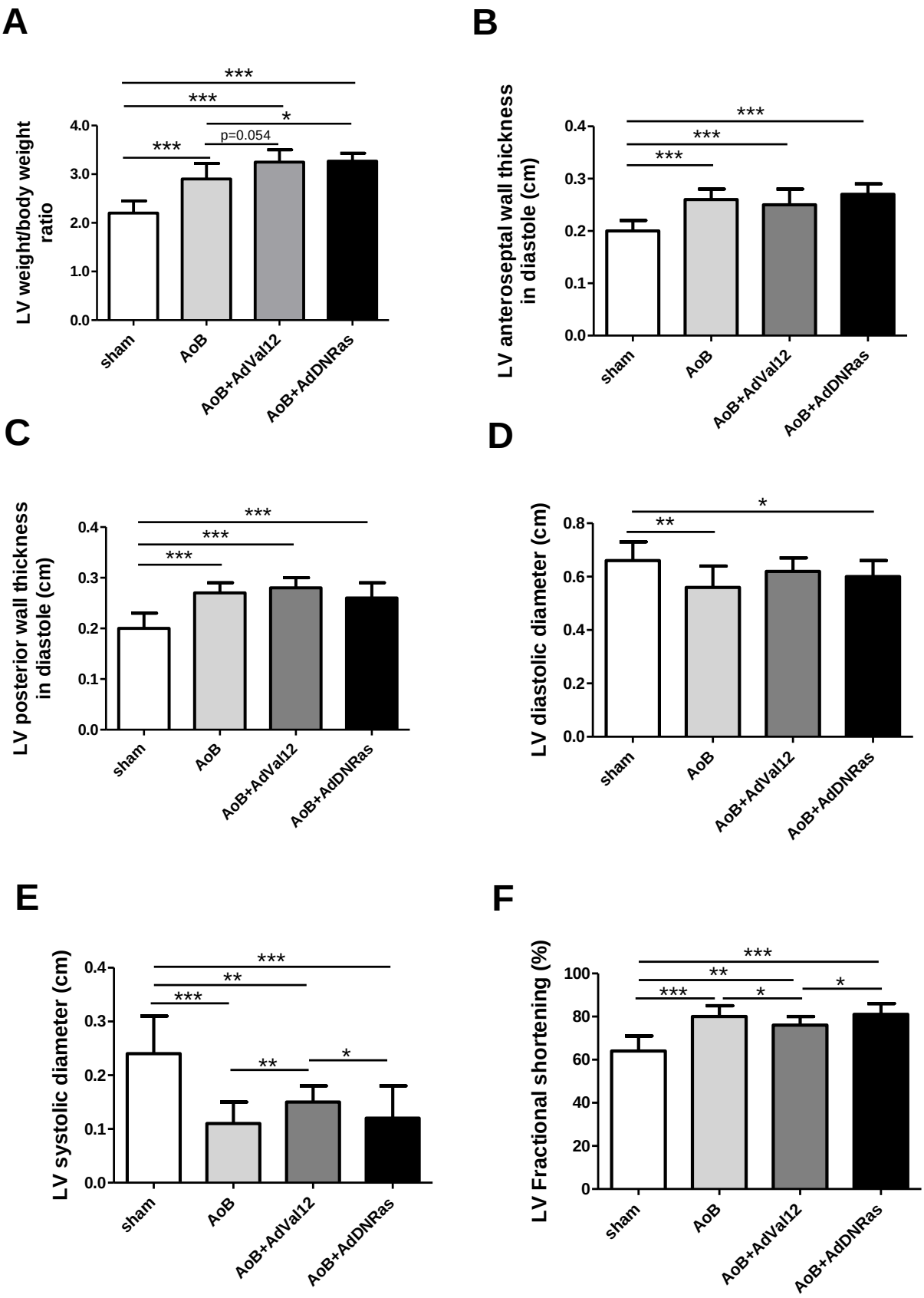
A
LV weight/body weight ratio
4.0
3.0
2.0
1.0
0.0
***
***
*
p=0.054
***
sham
AoB
AoB+AdVal12
AoB+AdDNRas
B
LV anteroseptal wall thickness in diastole (cm)
0.4
0.3
0.2
0.1
0.0
***
***
***
sham
AoB
AoB+AdVal12
AoB+AdDNRas
C
LV posterior wall thickness in diastole (cm)
0.4
0.3
0.2
0.1
0.0
***
***
***
sham
AoB
AoB+AdVal12
AoB+AdDNRas
D
LV diastolic diameter (cm)
0.8
0.6
0.4
0.2
0.0
*
**
sham
AoB
AoB+AdVal12
AoB+AdDNRas
E
LV systolic diameter (cm)
0.4
0.3
0.2
0.1
0.0
***
**
***
**
*
sham
AoB
AoB+AdVal12
AoB+AdDNRas
F
LV Fractional shortening (%)
100
80
60
40
20
0
***
**
***
*
*
sham
AoB
AoB+AdVal12
AoB+AdDNRas

Figure 6

A

Sarcomere shortening representative tracing

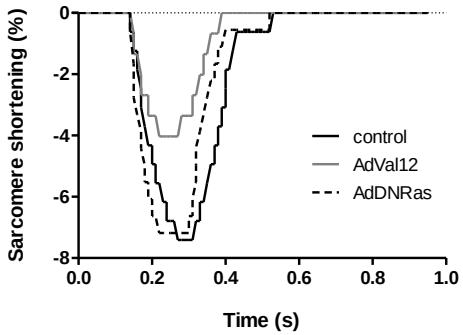

B

Sarcomere shortening, % of resting length

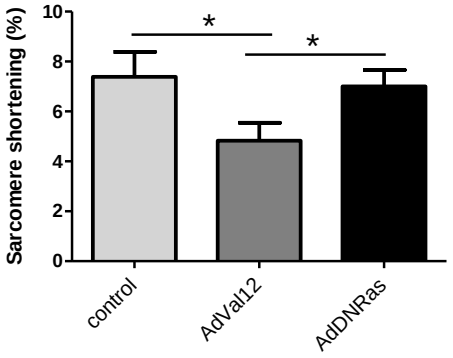

C

Sarcomere contraction half-time

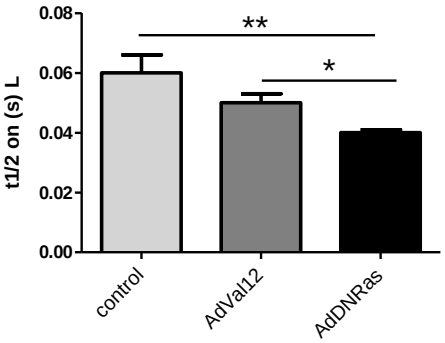

D

Sarcomere relaxation half-time

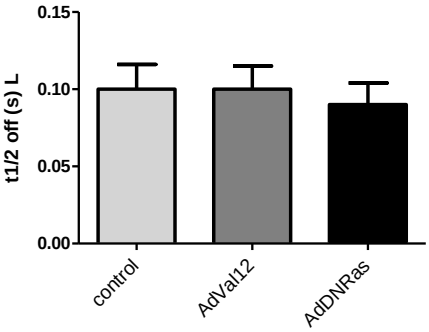

E

Calcium transient representative tracing

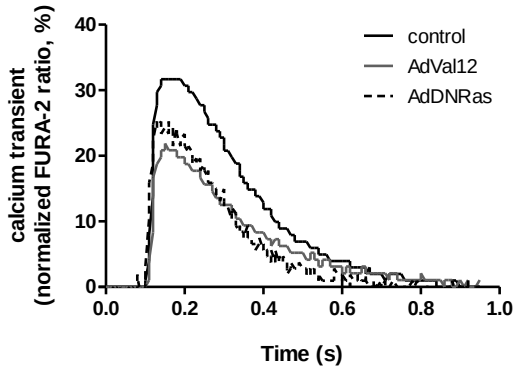

F

Calcium transient diastolic ratio

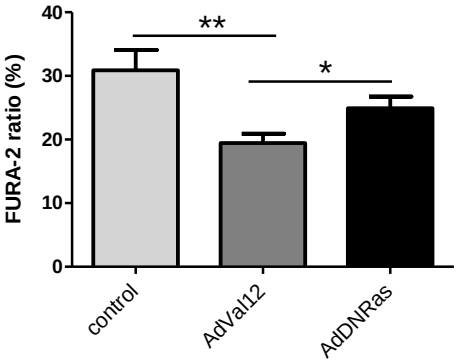

G

Caclium transient rising half-time

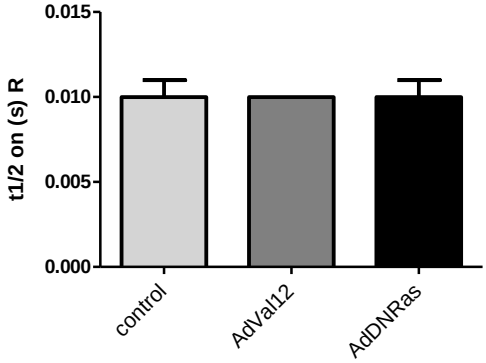

H

Calcium transient decay half-time

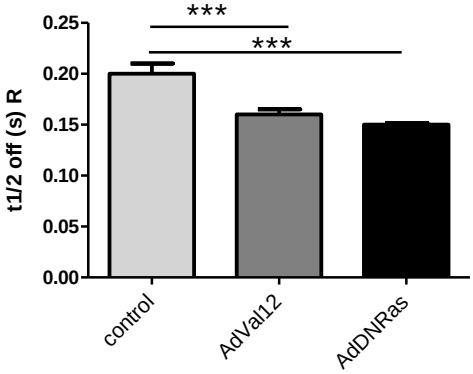

Figure 7.

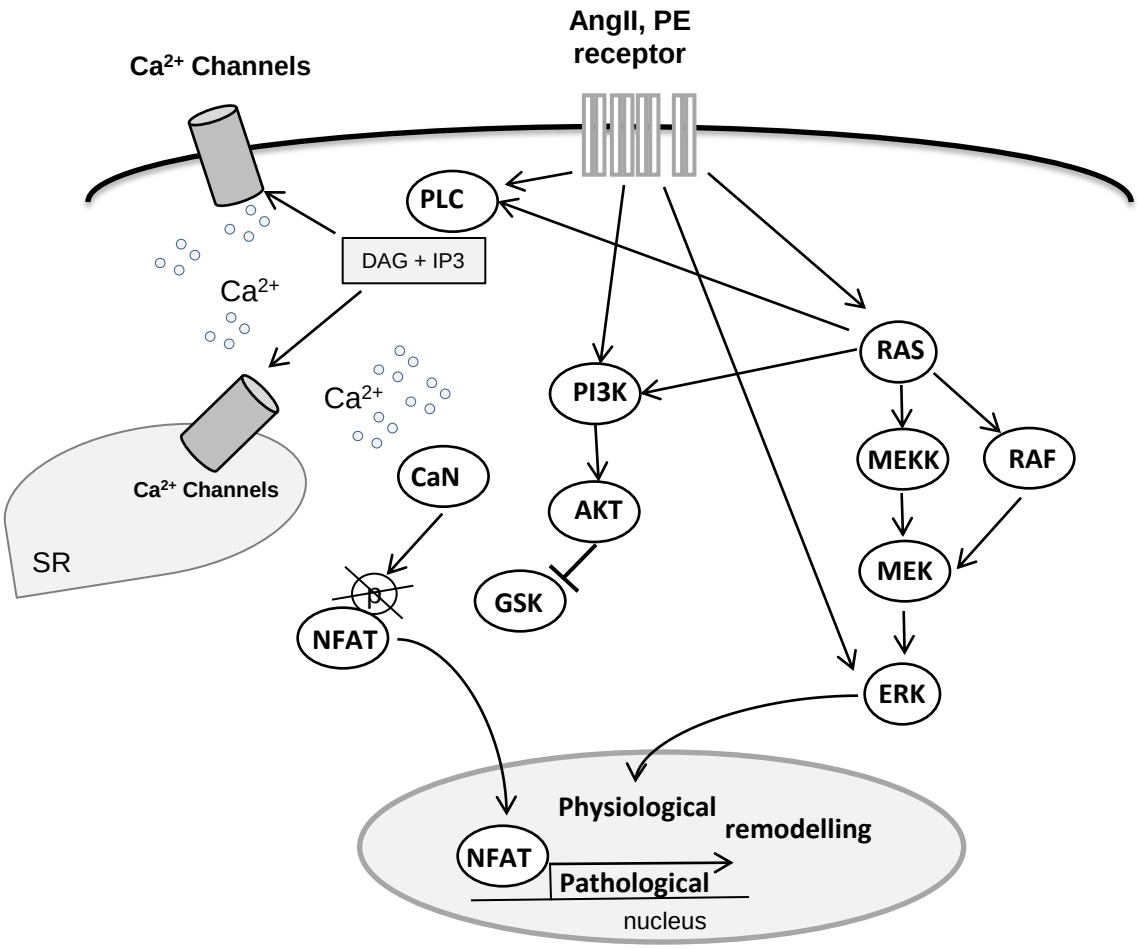
AngII, PE receptor
Ca2+ Channels
PLC
DAG + IP3
Ca2+
Ca2+
Ca2+ Channels
SR
CaN
NFAT
P
PI3K
AKT
GSK
RAS
MEKK
RAF
MEK
ERK
Physiological remodelling
NFAT
Pathological
nucleus

Figure 8

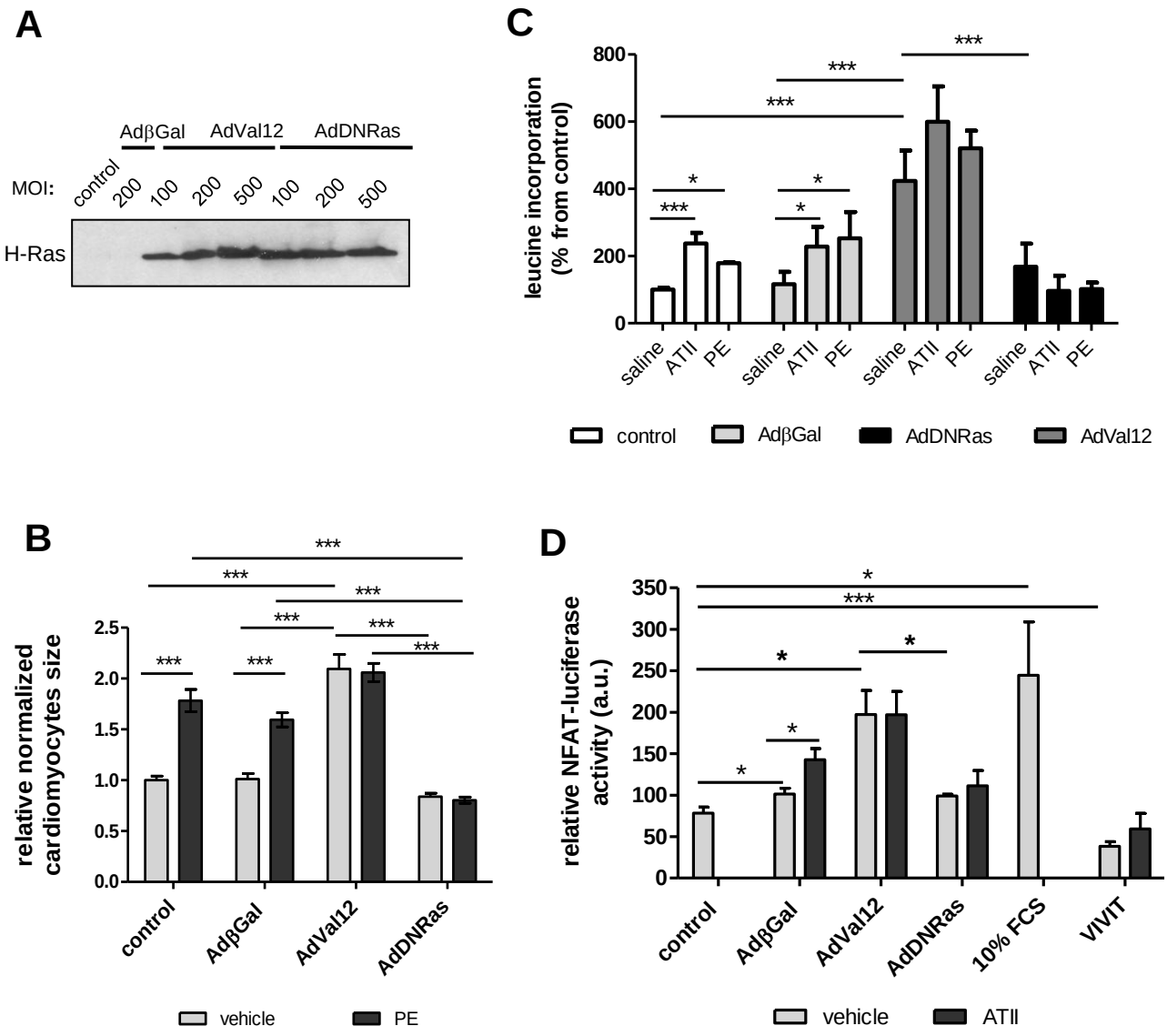
A
AdβGal
AdVal12
AdDNRas
MOI:
control
200
100
200
500
100
200
500
H-Ras
C
leucine incorporation (% from control)
800
600
400
200
0
***
*
saline
ATII
PE
control
AdβGal
AdDNRas
AdVal12
B
relative normalized cardiomyocytes size
2.5
2.0
1.5
1.0
0.5
0.0
control
AdβGal
AdVal12
AdDNRas
vehicle
PE
D
relative NFAT-luciferase activity (a.u.)
350
300
250
200
150
100
50
0
10% FCS
VIVIT
vehicle
ATII

Figure 1.

A

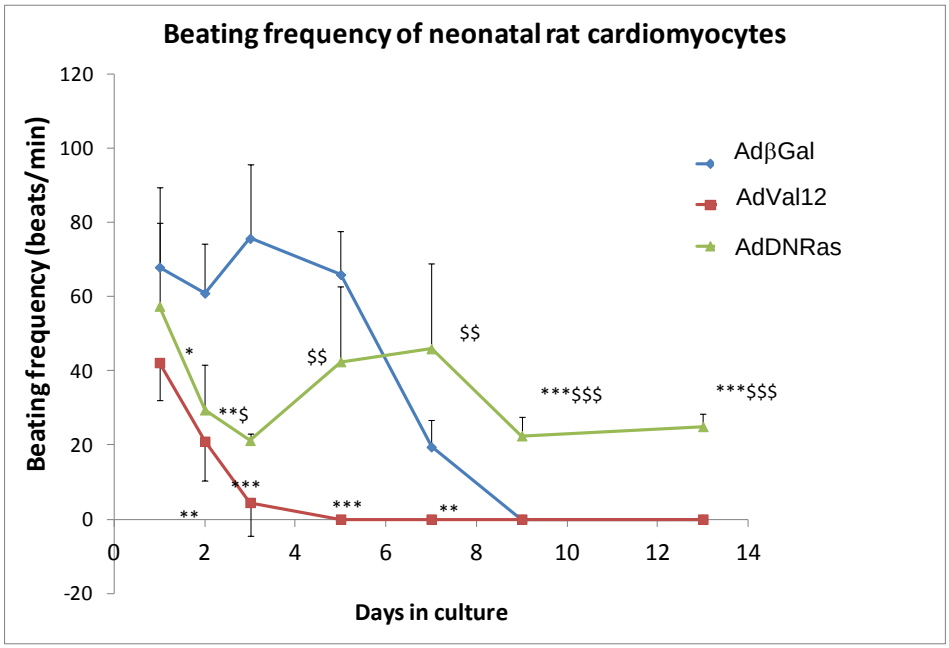

B

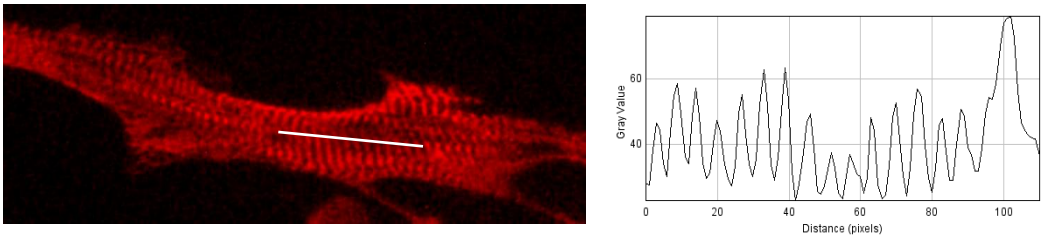

C

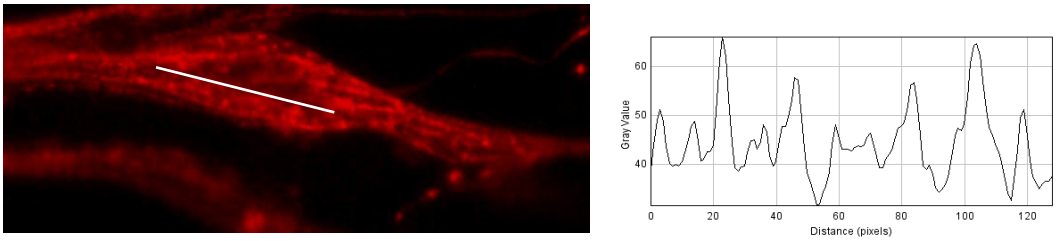

D

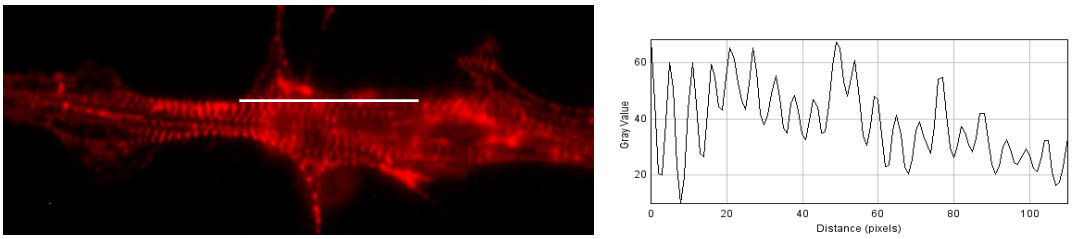

Figure 2.

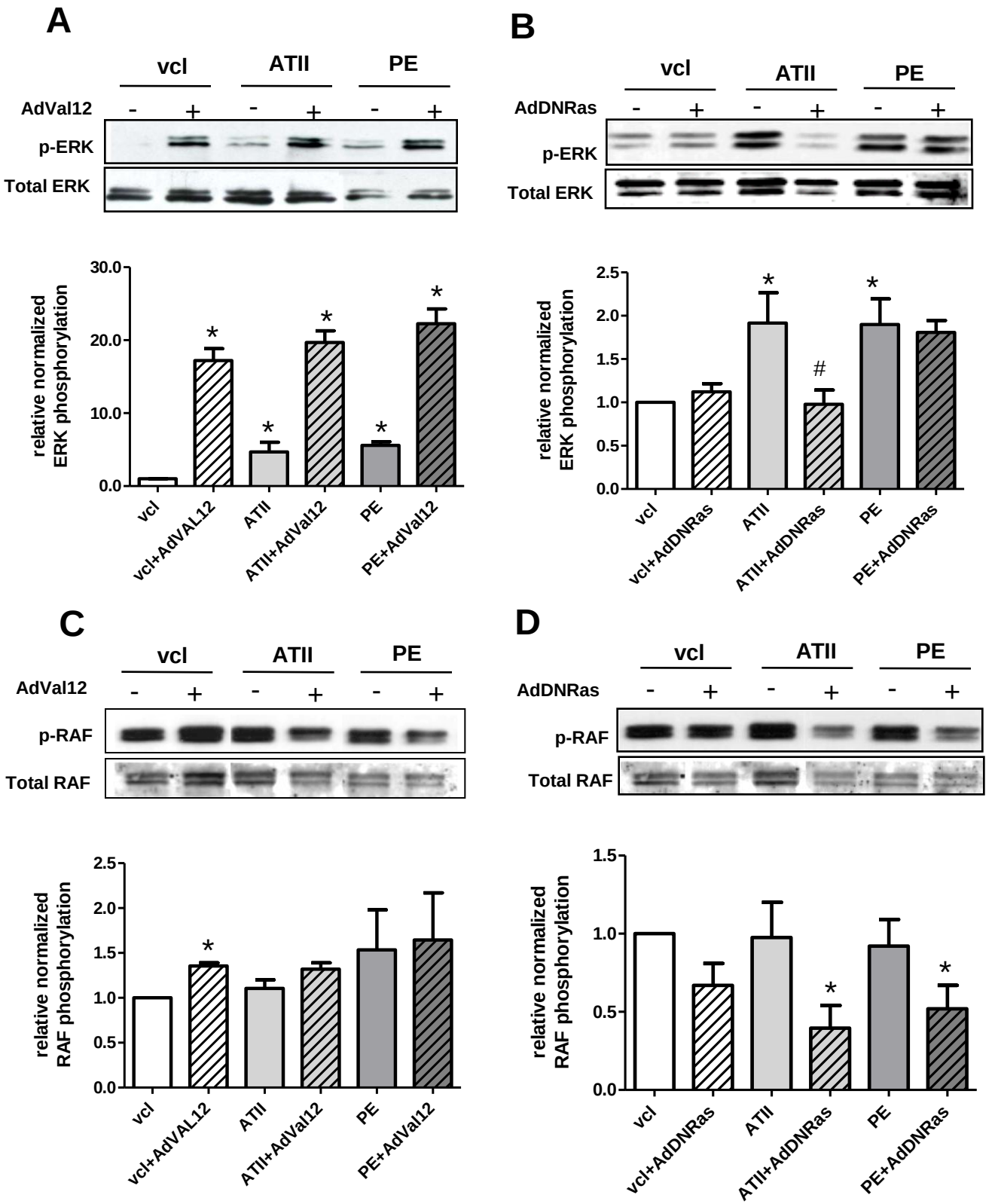
A
vcl
ATII
PE
AdVal12
- + - + - +
p-ERK
Total ERK
relative normalized ERK phosphorylation
30.0
20.0
10.0
0.0
vcl
vcl+AdVAL12
ATII
ATII+AdVal12
PE
PE+AdVal12
B
vcl
ATII
PE
AdDNRas
- + - + - +
p-ERK
Total ERK
relative normalized ERK phosphorylation
2.5
2.0
1.5
1.0
0.5
0.0
#
vcl
vcl+AdDNRas
ATII
ATII+AdDNRas
PE
PE+AdDNRas
C
vcl
ATII
PE
AdVal12
- + - + - +
p-RAF
Total RAF
relative normalized RAF phosphorylation
2.5
2.0
1.5
1.0
0.5
0.0
vcl
vcl+AdVAL12
ATII
ATII+AdVal12
PE
PE+AdVal12
D
vcl
ATII
PE
AdDNRas
- + - + - +
p-RAF
Total RAF
relative normalized RAF phosphorylation
1.5
1.0
0.5
0.0
vcl
vcl+AdDNRas
ATII
ATII+AdDNRas
PE
PE+AdDNRas

Figure 3.

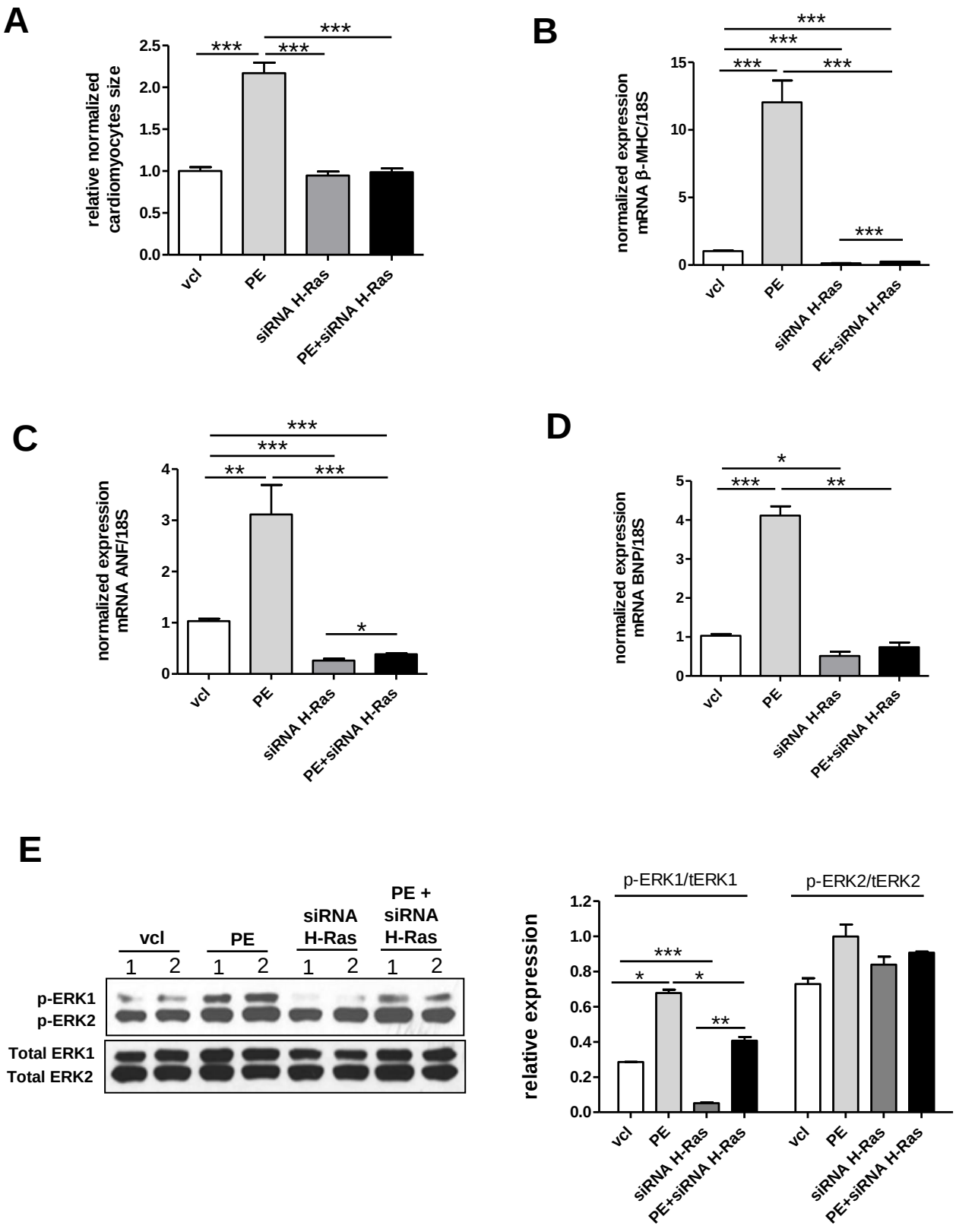
A
relative normalized cardiomyocytes size
2.5
2.0
1.5
1.0
0.5
0.0
***
***
***
vcl
PE
siRNA H-Ras
PE+siRNA H-Ras
B
normalized expression mRNA β-MHC/18S
15
10
5
0
***
***
***
***
***
vcl
PE
siRNA H-Ras
PE+siRNA H-Ras
C
normalized expression mRNA ANF/18S
4
3
2
1
0
***
***
**
***
*
vcl
PE
siRNA H-Ras
PE+siRNA H-Ras
D
normalized expression mRNA BNP/18S
5
4
3
2
1
0
*
***
**
vcl
PE
siRNA H-Ras
PE+siRNA H-Ras
E
vcl
PE
siRNA H-Ras
PE + siRNA H-Ras
1 2 1 2 1 2 1 2
p-ERK1
p-ERK2
Total ERK1
Total ERK2
p-ERK1/tERK1
p-ERK2/tERK2
relative expression
1.2
1.0
0.8
0.6
0.4
0.2
0.0
***
*
*
**
vcl
PE
siRNA H-Ras
PE+siRNA H-Ras
vcl
PE
siRNA H-Ras
PE+siRNA H-Ras

Figure 4.

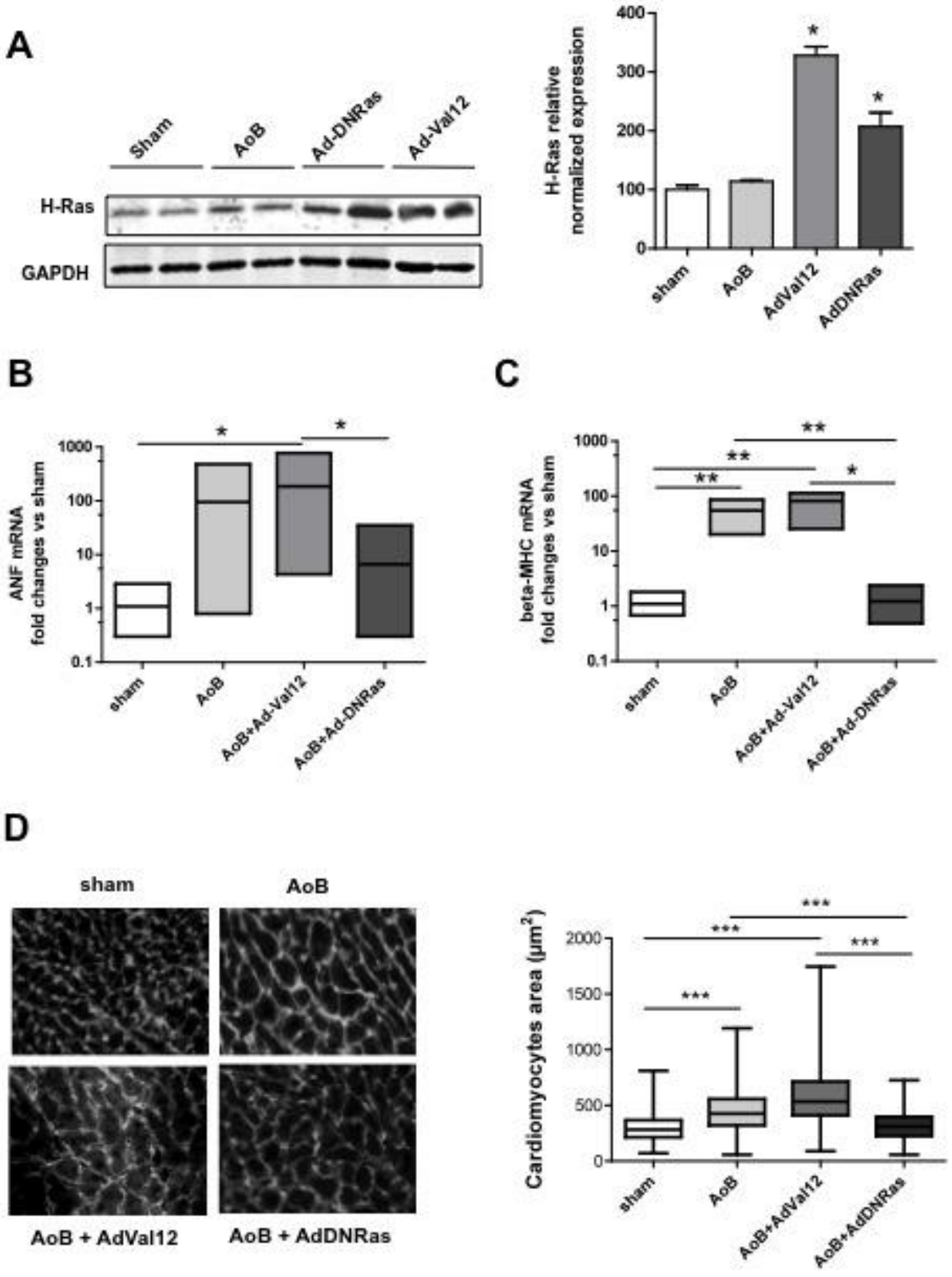
A
Sham
AoB
Ad-DNRas
Ad-Val12
H-Ras
GAPDH
H-Ras relative normalized expression
400
300
200
100
0
*
*
sham
AoB
AdVal12
AdDNRas
B
ANF mRNA fold changes vs sham
1000
100
10
1
0.1
*
*
sham
AoB
AoB+Ad-Val12
AoB+Ad-DNRas
C
beta-MHC mRNA fold changes vs sham
1000
100
10
1
0.1
**
**
**
*
sham
AoB
AoB+Ad-Val12
AoB+Ad-DNRas
D
sham
AoB
AoB + AdVal12
AoB + AdDNRas
Cardiomyocytes area (μm²)
2000
1500
1000
500
0
***
***
***
***
sham
AoB
AoB+AdVal12
AoB+AdDNRas

Figure 5.

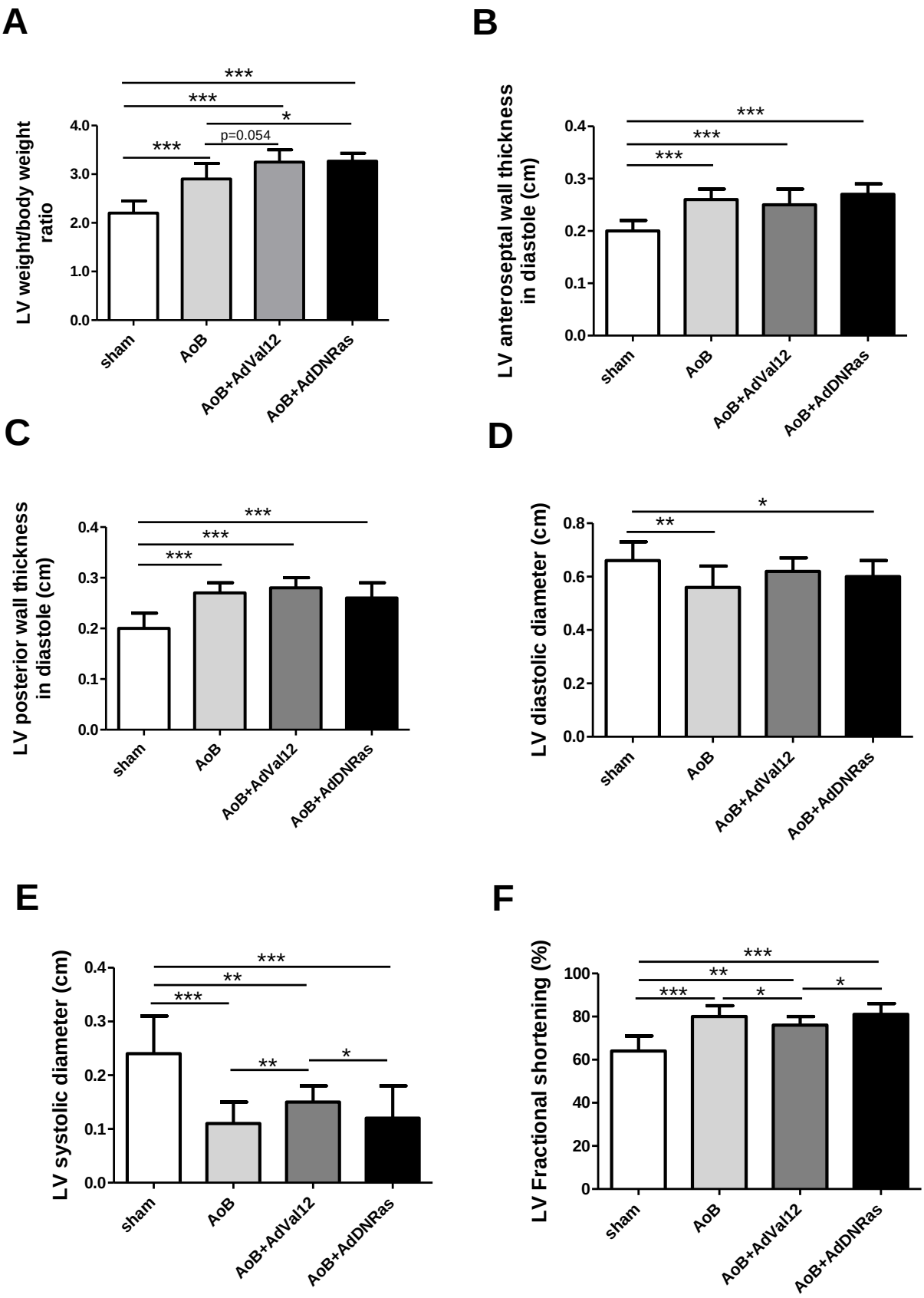
A
LV weight/body weight ratio
4.0
3.0
2.0
1.0
0.0
***
***
*
p=0.054
***
sham
AoB
AoB+AdVal12
AoB+AdDNRas
B
LV anteroseptal wall thickness in diastole (cm)
0.4
0.3
0.2
0.1
0.0
***
***
***
sham
AoB
AoB+AdVal12
AoB+AdDNRas
C
LV posterior wall thickness in diastole (cm)
0.4
0.3
0.2
0.1
0.0
***
***
***
sham
AoB
AoB+AdVal12
AoB+AdDNRas
D
LV diastolic diameter (cm)
0.8
0.6
0.4
0.2
0.0
*
**
sham
AoB
AoB+AdVal12
AoB+AdDNRas
E
LV systolic diameter (cm)
0.4
0.3
0.2
0.1
0.0
***
**
***
**
*
sham
AoB
AoB+AdVal12
AoB+AdDNRas
F
LV Fractional shortening (%)
100
80
60
40
20
0
***
**
***
*
*
sham
AoB
AoB+AdVal12
AoB+AdDNRas

Figure 6

A

Sarcomere shortening representative tracing

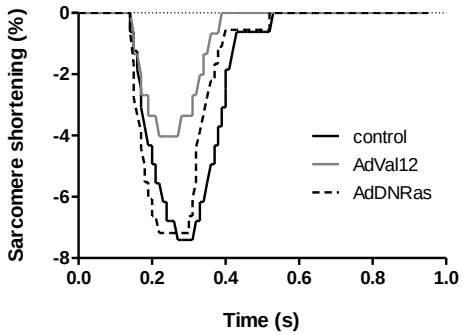

B

Sarcomere shortening, % of resting length

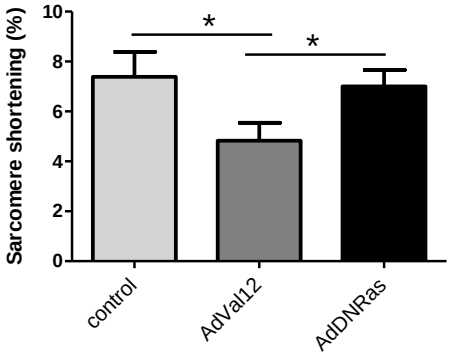

C

Sarcomere contraction half-time

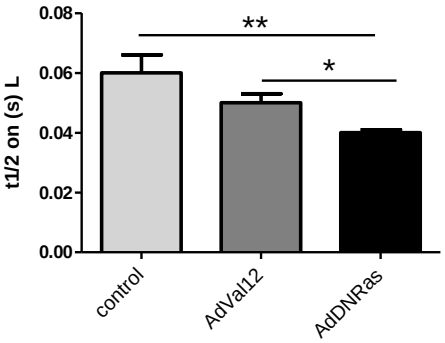

D

Sarcomere relaxation half-time

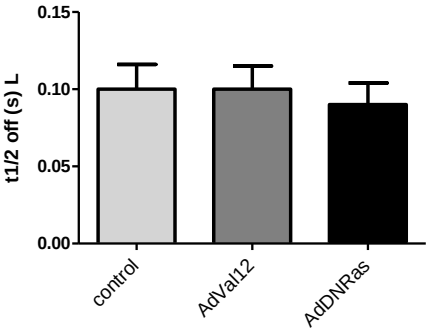

E

Calcium transient representative tracing

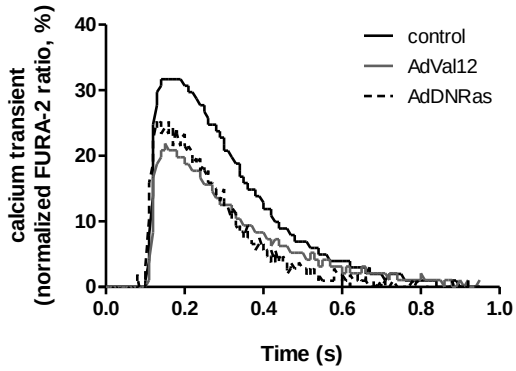

F

Calcium transient diastolic ratio

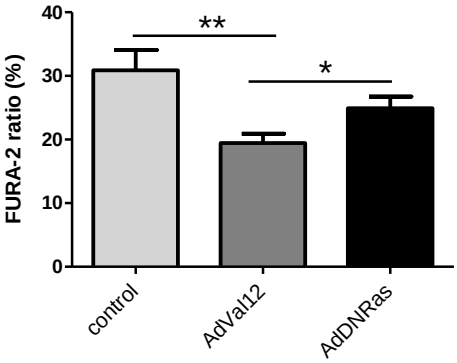

G

Caclium transient rising half-time

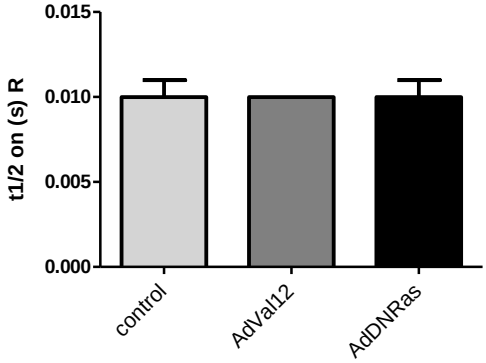

H

Calcium transient decay half-time

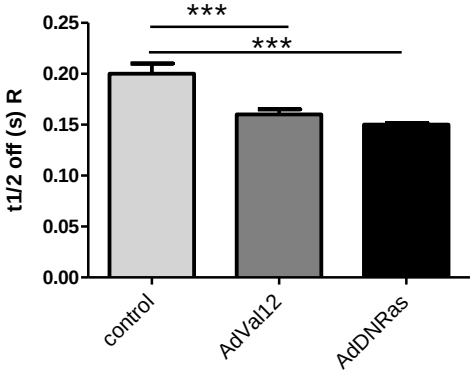

Figure 7.

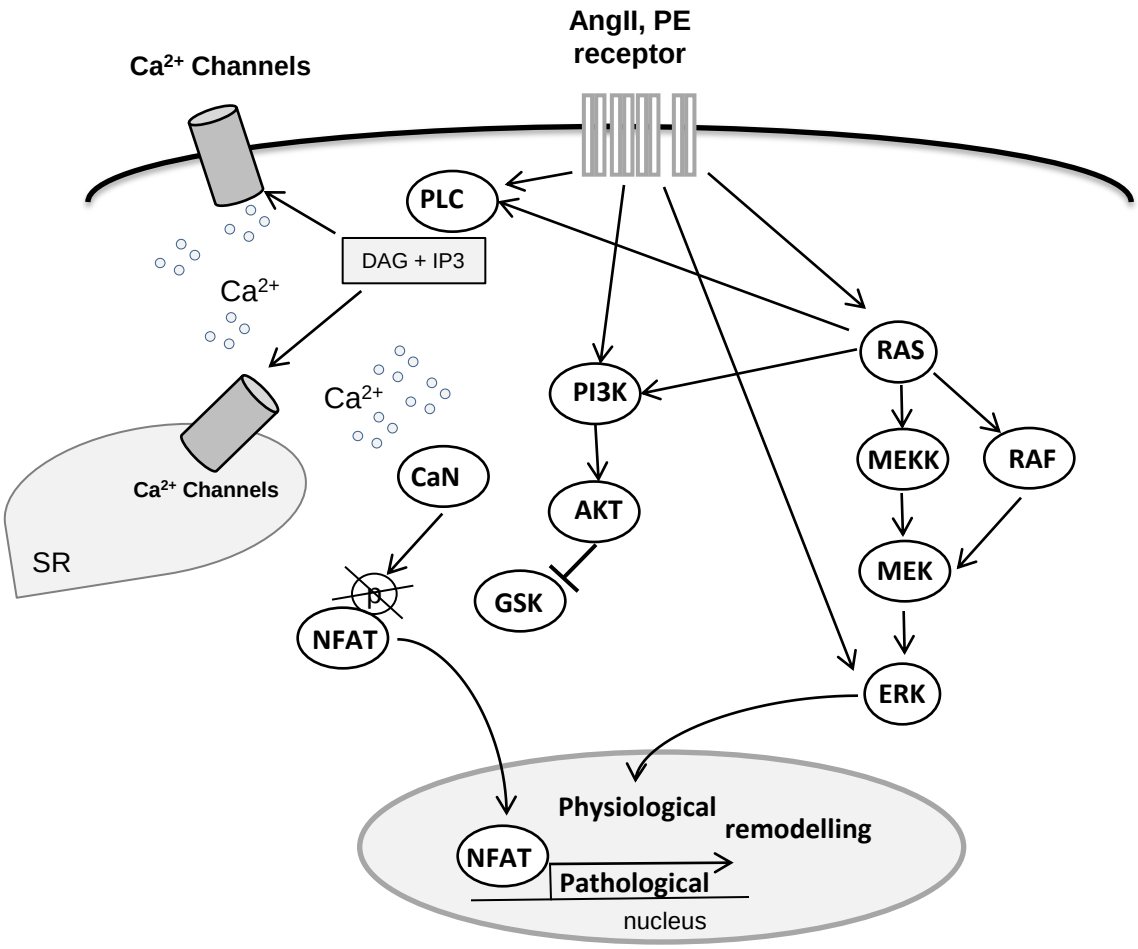
AngII, PE receptor
Ca2+ Channels
PLC
DAG + IP3
Ca2+
Ca2+
Ca2+ Channels
SR
CaN
NFAT
P
PI3K
AKT
GSK
RAS
MEKK
RAF
MEK
ERK
Physiological remodelling
NFAT
Pathological
nucleus

Figure 8